Chinese Journal of Chemical Engineering 26 (2018) 2238–2254

Contents lists available at ScienceDirect

Chinese Journal of Chemical Engineering

journal homepage: www.elsevier.com/locate/CJChE

Review

Recent advances in polymeric membranes for CO_2 capture

Yang Han, W.S. Winston Ho *

William G. Lowrie Department of Chemical and Biomolecular Engineering and Department of Materials Science and Engineering, The Ohio State University, 151 West Woodruff Avenue, Columbus, OH 43210-1350, USA

ARTICLE INFO

Article history:
Received 31 May 2018
Received in revised form 14 July 2018
Accepted 17 July 2018
Available online 2 August 2018

Keywords:
Carbon capture
Polymeric membrane
Gas separation

ABSTRACT

Membrane and membrane process have been considered as one of the most promising technologies for mitigating CO_2 emissions from the use of fossil fuels. In this paper, recent advances in polymeric membranes for CO_2 capture are reviewed in terms of material design and membrane formation. The selected polymeric materials are grouped based on their gas transport mechanisms, *i.e.*, solution-diffusion and facilitated transport. The discussion of solution-diffusion membranes encompasses the recent efforts to shift the upper bound barrier, including the enhanced CO_2 solubility in several rubbery polymers and novel methods to construct shape-persisting macromolecules with unprecedented sieving ability. The carrier-bearing facilitated transport membranes are categorized based on the specific CO_2-carrier chemistry. Finally, opportunities and challenges in practical applications are also discussed, including post-combustion carbon capture (CO_2/N_2), hydrogen purification (CO_2/H_2), and natural gas sweetening (CO_2/CH_4).

1. Introduction

Significant advances in polymeric membrane materials for gas separations have been witnessed in the past decade. Nearly hundreds of polymer materials have been engineered, and their unprecedented transport properties could enable an energy-efficient route for large-scale gas separations. These concerted research efforts are largely catalyzed by the urgent need to reduce CO_2 emissions from the usage of fossil fuels. CO_2 capture from fuel gases (*e.g.*, natural gas and syngas) and combustion flue gases (*e.g.*, coal-fired power plant flue gas) is generally believed to be the effective technological solution to mitigate the environmental and economic impacts of CO_2-induced climate change [1]. Compared to other CO_2 separation processes, membrane is advantageous for its system compactness, energy efficiency, operational simplicity, and ability to overcome thermodynamic solubility limitations [2]. These features stem from the fact that membrane is a thin interphase acting as a selective barrier separating two phases [3]. This thinness, typically in the range of 100 nm to a few micrometers, provides an almost natural platform to implement sophisticatedly engineered macromolecular structures.

In this review, opportunities and challenges in membrane-based carbon capture are discussed, including CO_2/N_2 separation in post-combustion carbon capture, CO_2/H_2 separation in syngas processing, and CO_2/CH_4 separation in natural gas sweetening. These separation scenarios differ in the CO_2 partial pressure. The post-combustion flue gases are typically discharged at atmospheric pressure with 11 vol%–15 vol% CO_2 for coal-fired power plants and 4 vol%–8 vol% for natural gas-fired power plants [4]. The low CO_2 partial pressure, along with the enormous volumetric flow rate, requires considerable CO_2 permeance and CO_2/N_2 selectivity to achieve bulk CO_2 removal with high product CO_2 purity [5,6]. In the syngas processing, the reforming of hydrocarbon produces a H_2-rich syngas with around 30 vol% CO_2 [7]. The CO_2/H_2 separation is typically performed after the water-gas shift reaction, where a pressure as high as 5 MPa yields a large transmembrane driving force, but a sufficiently high CO_2/H_2 or H_2/CO_2 selectivity is required to minimize the H_2 loss. Natural gas dehydration and sweetening are typically carried out at 3–6 MPa with 5%–70% CO_2 based on the geographical location, although the feed natural gas pressure can be as high as 35 MPa [8]. As a pressure driven process, membranes are well suited for these high pressure applications. However, the mechanical properties and the resistance to plasticization are of paramount importance for polymers in these separation scenarios [9].

Over the past decade, better polymeric materials with improved CO_2 permeability and selectivity have been extensively searched. However, a fundamental barrier is the permeability/selectivity trade-off, *i.e.*, more permeable polymers tend to possess less selectivity and *vice versa* [10]. This trade-off is deeply rooted in the solution-diffusion mechanism that most polymeric materials rely on [11]. Conventionally, this limiting behavior is represented by an empirical upper bound, which was firstly proposed by Robeson in 1991 [12] then updated in 2008 [13]. The recent efforts to shift the upper bound are discussed in this review, including the enhanced CO_2 solubility in several rubbery polymers and the novel methods to construct shape-persisting macromolecules with unprecedented sieving ability. One approach to overcome the upper bound is by incorporating reactive sites to facilitate

* Corresponding author.
E-mail address: ho.192@osu.edu (W.S.W. Ho).

https://doi.org/10.1016/j.cjche.2018.07.010
1004-9541/

the CO_2 transport. The facilitated transport membranes are also reviewed based on the specific CO_2-carrier chemistry.

One key requirement for a successful industrial gas separation membrane is the processability. Most CO_2 separation applications require the reliable production of a thin selective layer of 0.1–10 μm at a scale of 1000–1000000 m^2 membrane area. At such a scale, polymers are the preferable membrane materials and nearly all commercial membranes are made from polymers with good scalability and low cost. The membrane formation ability of the emerging polymers is discussed in this review. Perspectives and future research directions are provided to enable the use of polymeric membranes in commercial-scale gas separation processes.

It should be noted that another strategy to utilize the processability of polymers is to add inorganic materials to form nano-composites known as mixed-matrix membranes (MMMs). Due to the specific pore size and geometry of the inorganic materials, well-constructed MMMs are capable of overcoming the upper bound while simultaneously possessing good processability. While not the emphasis of this review, considerable progresses have been achieved by MMMs with new sieving materials such as metal–organic frameworks (MOFs). Comprehensive reviews on MMMs can be found elsewhere [14,15].

2. Gas Transport in Polymeric Membranes

Membrane separation relies on the membrane material's ability to control the permeation of different species. Driven by the partial pressure differential, the penetrant firstly dissolves in the membrane, diffuses down the chemical potential gradient, and desorbs to the downstream side. This well-accepted explanation of gas permeation is referred as the solution-diffusion transport mechanism, in which a separation is achieved by the difference in the amount of the penetrant that dissolves in the polymer and/or the diffusion rate of the penetrant through the polymer. Because of its unique chemical structure, CO_2 can reversibly react with a Brønsted base, *e.g.*, KOH, or a Lewis base, *e.g.*, amine. These reversible reactions can be implemented in the membrane as a reactive diffusion pathway for CO_2 permeation. Therefore, a thin polymer phase with reactive sites is typically termed as a facilitated transport membrane. Due to the different physical and chemical aspects, these two gas transport mechanisms are discussed in this section as a general understanding of the vast polymeric membrane materials in the literature.

2.1. Solution-diffusion transport mechanism

In the absence of reactive moieties, the light gas molecules firstly dissolve in the dense polymer phase, diffuse across the membrane, then desorb into the low pressure downstream. The kinetic factor of this process is characterized as the permeability coefficient (P_i), which can be written as the product of the solubility coefficient (S_i) and the diffusion coefficient (D_i) [16]

$$P_i = S_i \times D_i \tag{1}$$

The most commonly used unit for P_i is Barrer, where 1 Barrer $= 1 \times 10^{-10}$ cm^3 (STP)·cm·cm^{-2}·s^{-1}·(cm Hg)$^{-1}$. A more directly measurable property of a membrane is its permeance, which represents the flux of a penetrant per unit permeation driving force. Traditionally, the permeance is expressed in Gas Permeation Unit (GPU) (1 GPU $= 1 \times 10^{-6}$ cm^3 (STP)·cm^{-2}·s^{-1}·(cm Hg)$^{-1}$). Therefore, the permeability can be calculated as the permeance divided by the thickness of a dense and uniform membrane. In the case of asymmetric or thin-film composite membranes, the permeability is barely reported due to the difficulty of defining an effective membrane thickness. In other words, the permeability is an intrinsic property of the membrane (selective layer) material, while the permeance is a practical measure of the separation performance of a membrane in a given configuration.

The separation capability of the membrane is characterized by the ideal selectivity α_{ij}, which is the ratio of two gas permeabilities. By Eq. (1), it can be further expressed by a solubility selectivity (S_i/S_j) and a diffusivity selectivity (D_i/D_j)

$$\alpha_{ij} = \frac{S_i}{S_j} \times \frac{D_i}{D_j} \tag{2}$$

Therefore, the separation can be achieved by the difference in solubility and/or diffusivity. The solubility of light gases in polymer is largely determined by its condensability and its affinity to the membrane material. The penetrant condensability increases with increasing critical temperature [17]. The diffusion of a gas molecule in polymer arises from the free volume characteristics of the polymer. The chain-to-chain spacing and the chain segment random motion allow molecules with small kinetic diameter to diffuse through [13]. In typical polymers, the penetrant diffusivity increases with decreasing kinetic diameter, as well as increasing free volume.

Table 1 summarizes the physical properties of CO_2, N_2, H_2, and CH_4. CO_2 has a higher solubility than the other gases due to its higher critical temperature. Consequently, the solubility selectivity favors CO_2. CO_2 also has a smaller kinetic diameter than N_2 and CH_4, resulting in a favorable diffusivity selectivity. These two factors render a CO_2-selective feature for most CO_2/N_2 and CO_2/CH_4 separation membranes. For CO_2/H_2, however, the diffusivity selectivity favors H_2, a much smaller molecule. Therefore, the final CO_2/H_2 selectivity depends on the polymer design. CO_2-selective membranes, *e.g.*, Polaris® from MTR, typically contain CO_2-philic moieties to enhance the solubility selectivity, while H_2-selective membranes, *i.e.*, polybenzimidazole (PBI)-based membranes, utilize glassy polymers with size-sieving capability [18].

Table 1
Physical properties of CO_2, N_2, H_2, and CH_4 [19]

Gas	Kinetic diameter/nm	Critical temperature/K
CO_2	0.330	304.1
N_2	0.364	126.2
H_2	0.289	33.2
CH_4	0.380	190.6

2.2. Facilitated transport mechanism

In facilitated transport membranes, mass transfer can be enhanced by the reversible reaction between the penetrant and reactive carriers [20]. Similar to the solution–diffusion transport mechanism, the penetrant first dissolves in the polymer matrix on the upstream side, where it reacts with a carrier to form a reaction product. Given certain mobility, this reaction product transports down its concentration gradient. At the downstream side, the low partial pressure of the penetrant drives the reverse reaction of the reaction product, by which the penetrant is released and the carrier is regenerated. Adding onto the normal Fickian diffusion, the permeation rate of the reactive penetrant is greatly enhanced. On the other hand, penetrants that are inert to the carrier are largely rejected due to the lack of the reactive diffusion pathway. In CO_2 separation processes, CO_2 is usually chosen to be selectively removed because the acidic nature of CO_2 enables it capable of fast reaction kinetics with basic carriers [21].

Even though quite many inorganic and organic bases have been used as carriers for CO_2 facilitated transport, most successes are achieved by exploiting the rich amine-CO_2 chemistry. Therefore, the reaction mechanisms between CO_2 and amines are briefly discussed in this section. The reactivity of CO_2 derives from the high electron deficiency of the carbon bonded to the two highly electronegative oxygens. For primary and secondary amines with a lone electron pair on the nitrogen atom, the amine functions as a nucleophile, *i.e.*, a Lewis base, which

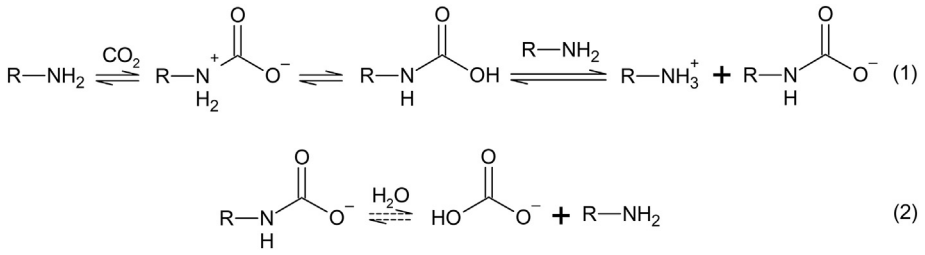

Fig. 1. CO_2 reaction with primary and secondary amines *via* the zwitterion mechanism.

attacks the electrophile carbonyl group on CO_2 to form a zwitterion. The zwitterion is rapidly deprotonated by another amine to form a more stable carbamate ion, which leads to 2 mol of amine for 1 mol of CO_2 (Reaction (1) in Fig. 1). At a lower pH, water can hydrate the carbamate species to produce bicarbonate and release a free amine (Reaction (2) in Fig. 1) [22]. The hydration reaction is considerably slow due to the stable structure of the carbamate. Unlike primary and secondary amines, a tertiary amine can only act as a Brønsted base, which neutralizes the carbonic acid formed by CO_2 in the presence of water (Fig. 2). This reaction involves 1 mol of amine for 1 mol of CO_2. This reaction, however, is known to be slow due to the slow formation of the carbonic acid [23].

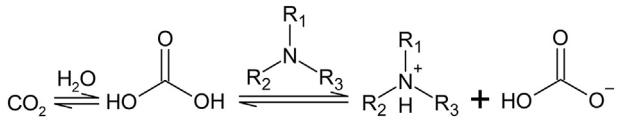

Fig. 2. CO_2 reaction with tertiary amine *via* acid–base reaction.

Fig. 3 depicts the transport of CO_2 *vs.* other inert light gases through an amine-containing facilitated transport membrane [24]. In this case, the amino groups are bound to the polymer backbone, and the CO_2 molecules hop among neighboring amino groups [24]. This hopping mechanism is an intramolecular diffusion in nature, which is also driven by the chemical potential gradient arising from the concentration gradient of carbamate ion [25]. The transport of non-reactive gases is governed by the solution–diffusion mechanism through a dense polymer matrix. Therefore, a high CO_2/gas (N_2, H_2 or CH_4) selectivity can be achieved.

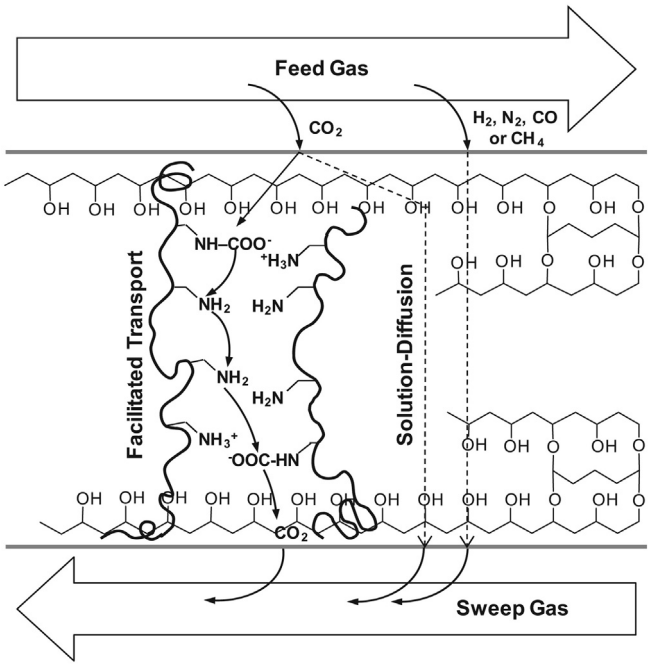

Fig. 3. Schematic diagram of gas transports through an amine-containing facilitated transport membrane.
(Adapted from Ref. [24] with permission from Elsevier.)

3. Solution-Diffusion Polymeric Membranes

In this section, the recent advances are discussed for polymers that are capable of selective CO_2 separation based on the solution-diffusion mechanism. Five classes of polymers are covered: poly(ethylene oxide) (PEO)-based polymers, perfluoropolymers, polymers of intrinsic microporosity (PIMs), thermally rearranged (TR) polymers, and iptycene-containing polymers. These classes are ordered based on when they were discovered or applied in gas separation. This sequence happens to coincide with the order of polymer chain stiffness, from the rubbery PEO to the glassy TR polymers. Strictly speaking, the iptycene-containing polymers are not a stand-alone category. Rather, they are derived/modified polymers *via* the incorporation of iptycene-containing moieties. The iptycene-containing polymers are discussed here individually, due to the uprising research efforts in this area.

3.1. PEO-based membranes

Even though CO_2 molecule is non-polar as a whole, the uneven distribution of charges inside grants the molecule a quadrupole moment [26]. The polar ether linkage (—C—C—O—) in poly(ethylene oxide) (PEO) is known to possess a high affinity to CO_2 *via* the quadrupole–quadrupole interaction [27]. Therefore, PEO-based polymers show a considerable CO_2 solubility, and the CO_2 selectivity mainly stems from the solubility selectivity. One drawback, however, is that the polar ether groups tend to form strong hydrogen bonding, which induces compact chain packing. A high degree of crystallinity has been reported in pure PEO or PEO-based materials [28]. The crystalline region limits the diffusion of CO_2 and eventually hampers the membrane permeability. The high crystallinity also leads to a weak mechanical strength, thus a poor film forming ability of PEO. To overcome these limitations, various approaches have been devised, including (1) block copolymerization with other hard segments, (2) blending with low MW poly (ethylene glycol) (PEG) and PEG-derivatives, and (3) crosslinking to form highly branched PEO polymer network. These concerted efforts not only produced considerably permeable PEO-based membrane materials, but also led to a deep understanding of the nanostructures of the PEO-based polymers. Table 2 summarizes the CO_2 permeabilities and CO_2/gas selectivities of the PEO-based polymers synthesized based on different strategies. The CO_2 permeances of a few membranes in thin-film composite configuration are also listed.

The most well-established approach to refrain the high crystallinity of PEO is to block copolymerize PEO with hard segments. The gas permeation properties of these copolymers are controlled by tuning the lengths of the soft and hard segments, as well as adjusting the fraction of the PEO phase in the copolymer. The first few groundbreaking copolymers were under the commercial names, Pebax® and Polyactive™, in which various polyamides (PA) and poly(butylene terephthalate) (PBT) served as the

Table 2
Transport properties of selected PEO-based polymers

Strategy	Material	$p(CO_2)$/atm	T/°C	$P(CO_2)$/Barrer	$\alpha(CO_2/N_2)$	$\alpha(CO_2/H_2)$	$\alpha(CO_2/CH_4)$
Copolymer	PEO-*b*-PA6 [19]	10	35	120	51.4	9.8	–
	PEO-*b*-PBT [29]	0.3	30	150	51.5	10.3	16.8
	PVC-*g*-POEM [30]	1	35	147	47	–	–
	PEO-*ran*-PPO-T6T6T [31]	4	35	470	43	10	13
	Pent-PI-PEO2000 [32]	3	35	39	36	4.1	–
	GPA1000-*g*-PEG-azide [33]	2	45	1840	36	8.3	–
	PEO-*b*-PBT on PDMS [34]	5	30	1815①	50	–	–
	PEO-*b*-PS [35]	1	70	20400①	27.7	–	–
Blending	PEO-PBT/PEG200 [29]	0.3	30	208	48.7	11.6	15.8
	PEO-PBT/PEG-BE [29]	0.3	30	400	50.1	11.8	12.5
	PEO-PBT/PEG-DBE [29]	0.3	30	750	40	12.4	11.2
	Pebax®1074/PEG1500 [36]	5	60	528	34.6	10.6	7.4
	Pebax® MH1657/PEGDME500 [37]	0.3	30	650	–	14.9	–
	Pebax® MH1657/PEG-AE [37]	0.3	30	335	–	12.9	–
	Pebax® MH1657/PEG-DVE [37]	0.3	30	570	–	12.9	–
	Pebax® MH1657/PEG-AME [37]	0.3	30	620	–	14.5	–
	PEO-PPO-T6T6T/PDMS-PEG [38]	4	35	896	36	10.6	10.9
	GPA1000/PEG-azide [33]	2	45	982	43	10.8	–
	Pebax®1657/PEGDME500 [39]	0.17	57	940①	30		
	Pebax® 2533/PEG-b-PPFPA [40]	3.5	35	940①	17	–	–
Crosslinking	PEGDA/PEGMEA [41]	4	35	570	41	–	–
	PEGDA/PEGMEA [42]	11	10	300	–	–	23
	PEGDA/TRIS-A [43]	15	35	716	19.9	7.7	–
	PAMAM/PEGDMA/4GMAP [44]	5.6	40	212	–	10	–
	TEGMVE/VEEM [45]	1	25	410	46	–	–
	PEO-526/dopamine/PEGDME [46]	3.5	50	200	30	6	10
	PEO-amine/PEO-epoxy [47]	3	35	376	53	10	–
	PEA/TMC [48]	0.2	25	360①	67.2	–	–
	DGBAmE/TMC [49]	0.71	22	1310①	33	–	–

$p(CO_2)$ = CO_2 partial pressure, 1 atm = 101.325 kPa; $P(CO_2)$ = CO_2 permeability; α = ideal CO_2/gas selectivity.
① Permeance measured in thin-film-composite membrane, GPU.

hard segments, respectively [19,29]. These PEO block copolymers typically showed a CO_2 permeability of 100–200 Barrers with a CO_2/N_2 selectivity around 50 at 25 °C. Recently, several novel hard segments were incorporated with PEO to synthesize ultra-permeable PEO-based copolymers, *e.g.*, monodisperse tetra-amide (T6T6T) [31] and pentiptycene-based polyimide (pent-PI) [32]. The self-assembly feature of the PEO-based block copolymer was also intensively studied. Yave *et al.* observed a polymer chain rearrangement when an ultrathin selective layer was coated onto a hydrophobic PDMS surface, leading to a high CO_2 permeance of 1815 GPU with a CO_2/N_2 selectivity of 50 at 30 °C [34]. A PEO–polystyrene (PS) block copolymer was synthesized by Xue *et al.* [35]. The copolymer self-assembled to form cylindrical PEO domains, which rendered an impressively high CO_2 permeance of 20400 GPU with a CO_2/N_2 selectivity of 27.7 at 70 °C [35].

Blending is another strategy to further increase the ether content in the polymer matrix. Short chain PEG, with a MW in the range of 100–2000, was fixed in PEO-based copolymer through polymer chain entanglement, which not only enhanced the CO_2 solubility, but also interrupted the compact packing of the PEO segment in the copolymer. The end groups on PEG also provided another control to mitigate the strong hydrogen bonding among the ether groups. For this reason, PEG moieties with terminal groups, such as methyl ether, ally ether, divinyl ether, and butyl ether, were studied [37]. Ultrathin composite membranes were also synthesized by this approach. Chen *et al.* reported a Pebax®-based membrane with poly(ethylene glycol)dimethyl ether (PEGDME-500) coated on deposited zeolite-Y nanoparticles [39]. The membrane demonstrated a CO_2 permeance of 940 GPU with a surprisingly high CO_2/N_2 selectivity of 30 at an elevated temperature of 57 °C.

The crosslinking method refers to the bottom-up synthesis of highly branched PEO or PEO-based copolymers through the polymerization of ethylene oxide monomer or oligomer. The initial work in this area was based on various methacrylate monomers, where the crosslinking reduced the crystallinity as well as improved the film forming ability [41]. Another interesting building block for the construction of PEO network is polyether terminated with amino groups. Jeffamine®, a commercially available polyether diamine, can react with multifunctional acyl chloride [48] or epoxide [47] through polycondensation reactions. A thin-film-composite membrane was synthesized by Li *et al. via* interfacial polymerization, which showed a CO_2 permeance of 1310 GPU with a CO_2/N_2 selectivity of 33 at 22 °C [49]. Recently, Kline *et al.* demonstrated that the crosslinking density and inhomogeneity could be tuned through the platform of polyether diamine and poly(ethylene glycol) diglycidyl ether [47]. Unimodal, bimodal and clustered PEO networks were synthesized (Fig. 4), and the inhomogeneous crosslinking improved the CO_2 permeability.

A special remark is needed for the membrane formation ability of PEO-based polymers. The rubbery nature of PEO bestows it a considerable solubility in most common organic solvents. These polymers can be readily coated on nanoporous substrate to form a sub-micron, defect-free selective layer. Significant advances have been achieved by Polaris® membranes from MTR to push the large-scale application in post- and pre-combustion carbon capture [50,51]. As one of the very few polymer materials that a high CO_2 permeance has been successfully demonstrated in thin-film-composite membranes under relevant testing conditions, PEO-based polymers have potential for commercialization. In addition, the several PEO-based materials that have shown viable selectivities at an operating temperature higher than 35 °C are of special interest [35,39]. The elevated temperature mitigates the intensive cooling associated with the membrane processes.

3.2. Perfluoropolymers

Perfluoropolymers are a class of glassy hydrocarbon polymers with most or all of its hydrogen atoms replaced by those of fluorine. Bestowed by the strong C—C and C—F covalent bonds, perfluoropolymers are resistant to most chemicals, which makes them ideal for applications that are subjected to hostile conditions [52]. The development of perfluoropolymers in gas separation, however, was largely hampered by their semi-crystalline nature and poor solvent processability. No gas permeation data were obtained until the introduction of several

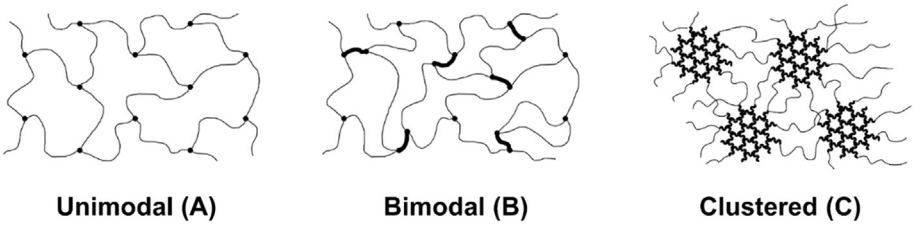

Fig. 4. Schematics of unimodal, bimodal, and clustered crosslinked PEO networks. (Adapted from Ref. [47] with permission from Elsevier.)

amorphous perfluoropolymers under the trade name Teflon™ AF, Hyflon™ AD, and Cytop™ in the mid-1980s. The chemical structures of these commercially available perfluoropolymers are shown in Fig. 5. They are either copolymers of tetrafluoroethylene and perfluorodioxole or cyclic homopolymers. These amorphous glasses are known for their high gas permeability due to the pre-existing microchannels [53]. Actually, the permeation data for these polymers defined the high permeability end of the 2008 Robeson upper bound for a number of important gas pairs [13]. The permselective properties of these commercial perfluoropolymers are listed in Table 3. Ranging from the most permeable Teflon™ AF2400 to the least permeable Cytop™, these glassy polymers generally show a H_2 selectivity over CO_2 and a CO_2 selectivity over CH_4. Stemmed from the overall low sorption for hydrocarbons, the low CH_4 permeability is of special interest since membranes can be tailored for separating He, H_2, CO_2, and N_2 from CH_4 in natural gas sweetening [54]. More importantly, the development of special fluorocarbon solvents, *e.g.*, Vertrel® XF and Novec™ 7200, has granted these polymers moderate solubilities, and thin-film-composite membranes have been synthesized. For instance, a Teflon™ AF2400 composite membrane was reported by Fang *et al.* with a CO_2 permeance of 13000 GPU and a CO_2/CH_4 selectivity of 5.7 [55]. The solvent processability allows the perfluoropolymers to be fabricated into a variety of composite membrane configurations. However, the cost and the toxicity of the specialty fluorocarbon solvents must be taken into consideration.

Noticeably, these highly permeable commercially available perfluoropolymers typically suffer from a moderate to low selectivity. Therefore, research efforts have been concerted to develop new fluorinated monomers for tunable polymer properties. Currently, most of the promising candidates fall into the category of perfluorodioxolane monomers, *e.g.*, perfluoro-(2-methylene-4-methyl-1,3-dioxolane) (PFMMD) and perfluoro-(2-methylene-1,3-dioxolane) (PFMD). Their homopolymers were synthesized, and improved selectivities were reported [59]. Interesting gas permeation results were also obtained for the copolymer of PFMMD and PFMD, where a high CO_2 permeance of 403 GPU with a considerable CO_2/CH_4 selectivity of 55 was reported at 22 °C [60]. Along with its potential chemical resistance, poly(PFMMD-*co*-PFMD) can be a well suited membrane material for removing CO_2 from natural gas. Further studies are needed regarding the high pressure plasticization, physical aging, and separation performance in the presence of hydrocarbon vapors. These issues have been somewhat investigated for the commercially available perfluoropolymers [61–64]. These studies suggested relatively slow physical aging of the perfluoropolymers.

3.3. Polymers of intrinsic microporosity (PIMs)

PIMs, firstly reported by Budd and McKeown [65], refer to a class of glassy polymers with rigid and contorted macromolecular backbone structure. Originated from the sites of contortion or spiro centers, the restricted chain rotation of the component macromolecules induces poor molecular packing, resulting in interconnected pores of less than 2 nm [66]. The intrinsic microporosity of this class of polymers results in a >20% fractional free volume (FFV), thereby an ultrahigh gas

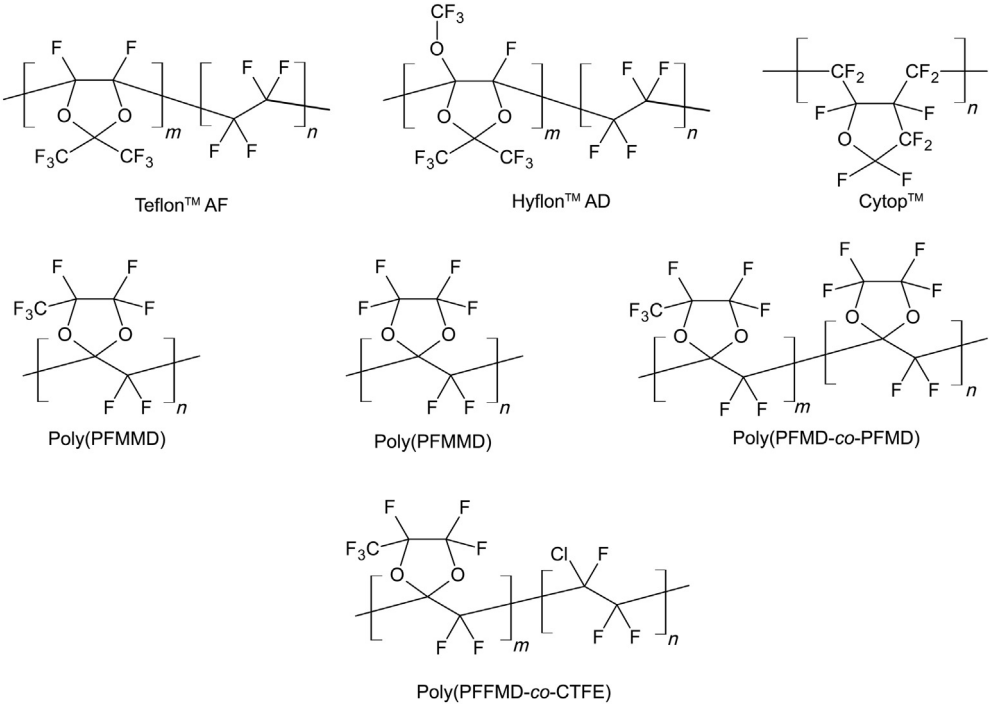

Fig. 5. Structures of perfluoropolymers. The detailed grades of Teflon™ AF and Hyflon™ AD depend on the ratio of tetrafluoroethylene to the copolymerized dioxole unit.

Table 3
Transport properties of selected perfluoropolymers

Strategy	Material	$p(CO_2)$/atm	T/°C	$P(CO_2)$/Barrer	α (CO_2/N_2)	α (H_2/CO_2)	α (CO_2/CH_4)
Commercial	Teflon™ AF2400 [56]	1	35	2200	4.6	0.96	5.6
	Teflon™ AF1600 [57]	1	35	520	4.7	1.06	6.5
	Hyflon™ AD80 [58]	3	35	473	6.1	1.19	9.6
	Hyflon™ AD60 [58]	3	35	124	7.3	1.63	15.5
	Cytop™ [58]	1	35	35	7.0	1.69	17.5
	Teflon™ AF2400 [55]	4.4	22	13000①	4.8	0.81	5.7
	Hyflon™ AD60 [55]	4.4	22	1330①	7.3	1.28	18
Homopolymer	Poly(PFMD) [59]	4.4	35	5.9	8.3	8.47	—
	Poly(PFMMD) [59]	4.4	35	58	7.5	4.1	—
Copolymer	Poly(PFMMD-*co*-PFMD) [60]	4.4	22	403①	9.1	2.9	55
	Poly(PFMMD-*co*-CTFE) [60]	4.4	22	44①	9.0	5.7	49

$p(CO_2)$ = CO_2 partial pressure, 1 atm = 101.325 kPa; $P(CO_2)$ = CO_2 permeability; α = ideal CO_2/gas selectivity.
① Permeance measured in thin-film-composite membrane, GPU.

permeability regardless of the processing conditions [67]. Unlike most other porous organic polymers, PIMs are solution-processable [65]. These features quickly catalyzed intensive research efforts to synthesize different PIMs to improve the gas permeability and selectivity. In this section, the newly developed PIMs are reviewed, including spirobiindane (SBI)-based PIMs, Tröger's base (TB)-based PIMs, polyimide (PI)-based PIMs, and some other variations. The efforts to address the fast physical aging by crosslinking are also briefly discussed. Transport properties of some representative examples are listed in Table 4.

The kinks in PIMs polymer backbone were firstly realized by introducing the SBI moiety with large pendant groups. SBI refers to a molecule with two indanes connected by a spiro carbon center. The SBI moiety is typically polymerized with a halogen-containing aromatic monomer, which leads to the first few PIMs that have been made into gas separation membranes, *e.g.*, PIM-1 and PIM-7 [68,69]. The gas permeation in PIMs obeys the solution-diffusion mechanism. The higher condensability and smaller size of CO_2 yield CO_2/N_2 and CO_2/CH_4 selectivities in the range of 10–20. The CO_2/H_2 selectivity, however, is at most 1–2 since the size sieving feature favors the diffusion of H_2. The SBI center could be replaced with a spirofluorene (SBF) unit, and the resultant PIM-SBF exhibited less chain flexibility, yielding a very high CO_2 permeability of 13900 Barrers with a CO_2/CH_4 selectivity of 12.6 [70]. Recently, bulky tetramethyltetrahydronaphthalene (TMN) units were fused to the SBI units in PIM-1. The further reduced conformational flexibility led to a CO_2 permeability of 17500 Barrers with a CO_2/CH_4 selectivity of 8.3 [71].

Unlike the dibenzodioxane-forming reaction utilized by the SBI-based PIMs, chemistry based on Tröger's base (TB) has been undertaken to incorporate this rigid bicyclic unit into PIMs. In this reaction scheme, diamino aromatic polymers with bicyclic rings, *e.g.*, ethanoanthracene (EA) and triptycene (Trip), are fused with or without SBI centers to form a highly contorted network. In PIM-EA-TB, a TB-based PIM without the spiro centers, the chain rigidity was realized by the combined kinks from the fused rings [72]. In addition, the TB group provides additional Langmuir affinity toward CO_2, which is beneficial for improving the CO_2 selectivity [86]. Aiming for an even higher free volume, non-planar iptycene units have been used to replace EA to further disrupt the chain packing. A triptycene-based PIM with TB units was synthesized by Carta *et al.*, demonstrating a very high CO_2 permeability of 9709 Barrers with a CO_2/CH_4 selectivity of 10.7 [73].

The formation of imide *via* the polycondensation of anhydrides and diamines has also been employed in the synthesis of PIMs, termed as PI-based PIMs. The contortion sites can be within either the dianhydride [74] or the diamine [75]. It should be noted that the imide linkage does not contain any fused ring structure to refrain the chain rotation. For this reason, aromatic diamine monomers are typically used in the PI-based PIM synthesis to inhibit the conformational rearrangement [87]. The relatively flexible imide linkage also improves the polymer solubility in organic solvents, by which the established membrane formation methods may apply to this type of PIMs.

Aside from exploiting different chemistry for PIM synthesis, it is worth mentioning that several improved PIMs have been reported by

Table 4
Transport properties of selected PIMs

Strategy	Material	$p(CO_2)$/atm	T/°C	$P(CO_2)$/Barrer	α (CO_2/N_2)	α (CO_2/H_2)	α (CO_2/CH_4)
SBI-based PIMs	PIM-1 alcohol treated [68]	1	30	11200	18.4	3.4	9.7
	PIM-7 [69]	0.2	30	1100	26.0	1.3	17.7
	PIM-SBF [70]	1	25	13900	17.7	2.2	12.6
	PIM-TMN-SBI [71]	1	25	17500	16.2	2.4	8.3
TB-based PIMs	PIM-EA-TB [72]	1	25	7140	13.6	0.92	10.2
	PIM-SBI-TB [69]	1	25	2900	12.5	1.3	6.4
	PIM-Trip-TB [73]	1	25	9709	15.9	1.2	10.7
PI-based PIMs	PIM-SBI-PI [74]	1	25	8210	18.7	3.1	9.8
	PIM-EA-PI [75]	1	25	7340	19.9	1.7	16.1
	6FDA-DAT1-OH [76]	2	35	47	25.9	0.37	50
PIMs wo SBI	PIM-TMN-Trip [71]	1	25	33300	14.9	2.0	9.7
	PIM-HPB [77]	1	25	1800	20.0	2.7	10.5
Crosslinking	TOX-PIM-1 (thermal) [78]	4	22	5100	18.1	1.7	16.9
	PIM-1 (UV) [79]	4	22	6374	21.6	2.1	16.2
	PAH-PIM-1 (chemical) [80]	1	20	150	22.1	—	—
Blending	C-PIM-1/Matrimid® [81]	3.5	35	2268	18.7	1.4	13.3
	PIM-1/Ultem [82]	3.5	35	3276	21.1	—	11.8
	PIM-1/POSS–PEG [83]	1	30	1309	31	—	30
	PIM-1/HCP [84]	2	25	19086	11.6	—	—
Membrane	PIM-1 HF [85]	6.9	35	360①	27.7	1.0	22.5

$p(CO_2)$ = CO_2 partial pressure, 1 atm = 101.325 kPa; $P(CO_2)$ = CO_2 permeability; α = ideal CO_2/gas selectivity.
① Permeance measured in hollow-fiber membrane, GPU.

incorporating bulky side groups containing aromatic rings. For instance, the hexaphenylbenzene (HPB) unit is proven to interrupt the chain packing in PIMs, and the enhanced rigidity mitigates the physical aging [77]. A record-breaking CO_2 permeability of 333,000 Barrers with a CO_2/CH_4 selectivity of 9.7 was reported by Carta *et al.* by combining bulky TMN and Trip into PIM [71]. These PIMs have shown CO_2/N_2 separation performances surpassing the 2008 Robeson upper bound.

Like other glassy polymers with high free volume, PIMs are plagued by physical aging, where the relaxation of nonequilibrium chain conformations results in the loss of permeability over time [88]. One heavily studied approach is crosslinking to create a more robust polymer network. Thermal, UV, and chemical crosslinking methods have been reported for PIM-1. Song *et al.* reported a thermal oxidative crosslinking of PIM-1 in the presence of trace amount of oxygen. Stabilized permeation properties was observed over a period of one year [78]. A UV-induced crosslinking was also reported by the same research group to enhance the gas selectivities [79]. Several crosslinkers have also been used, such as polyethylene glycol biazide [89] and pyrene [80]. McDonald *et al.* reported a PIM-1 membrane crosslinked by 1-aminopyrene, where the pore size decreased over time and the CO_2 sorption was enhanced [80].

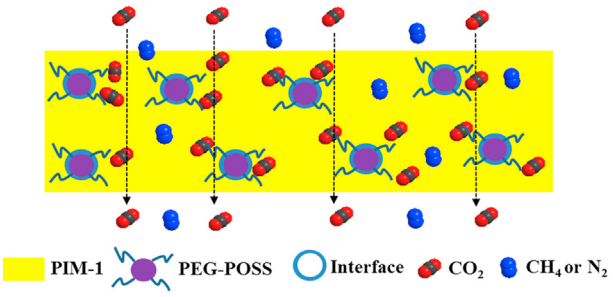

Fig. 6. Schematic of PIM-1/POSS–PEG.
(Adapted from Ref. [83] with permission from Elsevier.)

Despite the intensive research of PIMs on the aspect of material synthesis, studies of membrane formation are still in the early stage. On the one hand, the CO_2/gas (N_2 and CH_4) selectivities of most PIMs are lower than those offered by PEO-based membranes. Whether these highly permeable but only mediocrely selective materials suit the actual CO_2/N_2 or CO_2/CH_4 separation is debatable. On the other hand, the complicated synthesis route of PIMs adds additional cost onto membrane fabrication. A high membrane cost hampers applications in energy-related industries where the luxury to produce high-value chemicals does not exist. Driven by these reasons, other polymeric materials have been blended with PIMs to increase the gas selectivity as well as reduce the fabrication cost. Chung's group has dispersed PIM-1 or carboxylate PIM-1 in Ultem [82] and Matrimid® [81] as highly permeable nanofillers. Contrarily, PIM-1 has been used as the continuous phase by Yang *et al.* to bear nano-sized poly(ethylene glycol) functionalized polyhedral oligomeric silsesquioxane (POSS–PEG) [83]. Both approaches led to an increased CO_2/N_2 or CO_2/CH_4 selectivity, which was however compromised by a proportionally reduced CO_2 permeability. Interestingly, a high CO_2/CH_4 selectivity of 30 was reported for PIM-1/POSS–PEG with 10% of filler loading, which was significantly higher than the other PIM-based materials. The schematic of this membrane is shown in Fig. 6. Blending can also retard the physical aging of PIMs [88]. Hypercrosslinked polystyrene (HCP) was dispersed in PIM-1 as a filler phase [84]. The addition of HCP enhanced the CO_2 permeability to 19086 Barrers as well as slowed down the physical aging.

In terms of membrane formation, reports of PIM membranes in common thin-film-composite or hollow-fiber (HF) configuration are very limited. Recently, Jue *et al.* reported a defect-free HF asymmetric PIM-1 membrane prepared by phase inversion [85]. A skin-layer thickness of 3–6 μm was produced, and a CO_2 permeance of 360 GPU with a CO_2/CH_4 selectivity of 22.5 was obtained (Fig. 7). Structural designs that

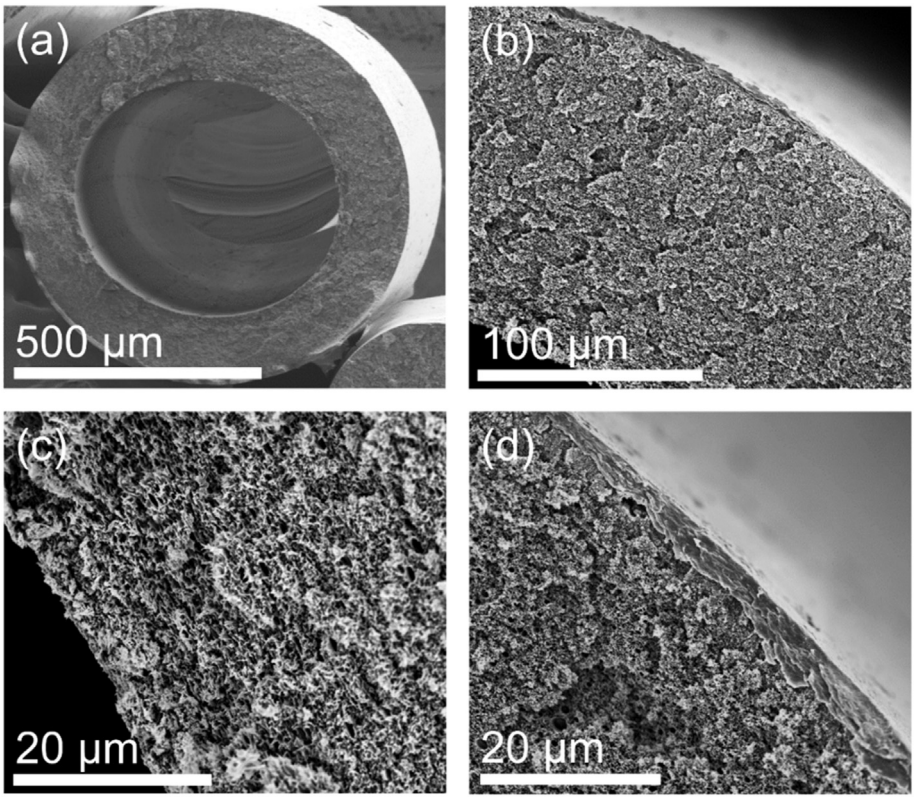

Fig. 7. SEM images of a defect-free PIM-1 hollow fiber (a) cross section, (b) asymmetric substructure, (c) internal boundary, and (d) skin layer.
(Adapted from Ref. [85] with permission from Elsevier.)

are amenable to large-scale applications are needed to capture PIM's potential as a high performance membrane material.

3.4. Thermally rearranged (TR) polymers

In comparison with the three-dimensional contorted chains of PIMs, more rigid and planer macromolecules can be formed by the thermally rearrangement of *ortho*-functionalized polyimides (PIs) or polyamide (PAs). First reported by Park *et al.*, this class of macromolecules is referred as thermally rearranged (TR) polymers [90]. The microporous nature arises from the high torsional energy barrier against rotation between the phenylene-heterocyclic rings. Therefore, the TR polymers are typically featured with unprecedented polymer chain rigidity and a narrow cavity size distribution. As shown in Fig. 8, the major precursors for the TR conversion are *ortho*-functionalized PIs or PAs. Upon a high temperature above 350 °C, an intramolecular cyclization is initiated, and a rigid polymer, *e.g.*, polybenzoxazole (PBO), polybenzimidazole (PBI) or polypyrrolone (PPL), is formed if the *ortho*-functional group is hydroxyl or amino [91]. The TR polymers derived from the polycondensation of dianhydride and *ortho*-functional diamine are termed as TR-α, while the ones from the polycondensation of hydroxy-diamine and diacid chloride are referred as TR-β.

Table 5 summarizes the transport properties of several selected TR polymers. The flexible hydroxyl group on the PA-precursor as well as the less bulky diacid chloride moiety renders TR-β a *ca.* 100 °C lower TR conversion temperature than TR-α. More importantly, the smaller cavity size also causes a lower permeability, as shown in Table 5 for the TR-β-PBO [90,92]. Regardless, the CO_2 permeability can be tuned spanning 3 orders of magnitude. Specially, the CO_2/CH_4 selectivity can be as high as 40–50 with decent CO_2 permeability, projecting a promising application of TR polymers in natural gas sweetening. A recent research focus is to use precursors with an even higher free volume. One example is shown in Fig. 9 for the bulky 2,2-bis(3-amino-4-hydroxyphenyl) adamantane (ADHAB) monomer synthesized by Aguilar-Lugo *et al.* [93]. The bulky adamantane group was proven to be thermally stable at the TR conversion temperature and led to CO_2 permeability and CO_2/CH_4 selectivity exceeding the 2008 Robeson upper bound.

Even though the high polymer chain rigidity grants TR polymers less tendency for physical aging, plasticization is still a pressing issue, especially for high pressure gas separation applications, such as natural gas sweetening. The widely investigated approach is the intermolecular crosslinking during thermal conversion. The primary crosslinking method is to incorporate 3,5-diaminobenzoic acid in the *ortho*-hydroxy PI precursors, followed by a mono-esterification reaction with diol [97]. The rigid linkages created by the crosslinking reaction can also increase the cavity size and free volume, which benefit the CO_2 permeability and selectivity [98].

Copolymerization of TR polymers with other functional segments that are not capable of the cyclic rearrangement is another competitive approach to tune the chain rigidity. Scholes *et al.* copolymerized a series of TR-α-PBI with 2,3,5,6-tetramethyl-1,4-phenylenediamine (4MPD) or 9,9′-bis(4-aminophenyl)fluorene (FDA), which were monomers that

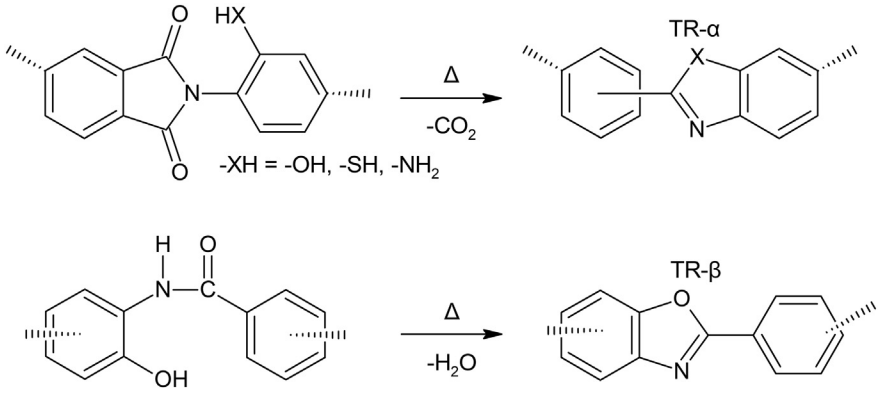

Fig. 8. Thermal rearrangement of (1) TR-α, where the precursor is an *ortho*-functional polyimide (PI) and (2) TR-β, where the precursor is an *ortho*-functional polyamide (PA).

Table 5
Transport properties of selected TR polymers

Strategy	Material	$p(CO_2)$/atm	T/°C	$P(CO_2)$/Barrer	$\alpha(CO_2/N_2)$	$\alpha(CO_2/H_2)$	$\alpha(CO_2/CH_4)$
TR-α-PBO	6FDA + bisAPAF [90]	10	35	4045	25.9	1.4	55.4
	6FDA + bisAPAF [94]	1	25	4201	14.8	1.0	27.8
	6FDA + bisAPAF + ADHAB [93]	3	30	151	21	–	42
	6FDA + HAB [95]	1	35	2.9	29	0	48.3
TR-α-PBI	6FDA + DAB [96]	1	25	1624	26.2	0.91	46.4
TR-β-PBO	BPDC + bisAPAF [92]	10	35	532	17.6	1.0	18.4
Crosslinking	6FDA + bisAPAF + DABA/diol [97]	1	25	746	25.2	1.2	37.5
	6FDA + bisAPAF + DABA [98]	1	25	491	24.3	1	37.8
Copolymer	6FDA + bisAPAF + DAM [99]	–	35	173	21.6	0.78	36
	6FDA + HAB + 4MPD [100]	10	35	226	10.5	–	39
	6FDA + bisAPAF + DAB [101]	1	25	1805	21.2	0.62	39.2
	6FDA + bisAPAF + DAB [101]	1	25	525	29.2	0.31	78.4
TR-labile PI	6FDA + DABA + βCD [102]	10	35	2707	15.3	0.34	17.3
	6FDA + durene + DABA + γCD [103]	2	35	1024	18.2	0.24	22.4
TR w/ SBI	TR-PIM-1 [104]	1	35	675	23	1.6	20
	TR-PIM-2 [104]	1	35	263	24	1	18
TR HF	6FDA + bisAPAF [105]	1	25	2326①	20	1.2	22
	6FDA + bisAPAF [106]	1	25	2500①	16	1.2	22

$p(CO_2)$ = CO_2 partial pressure, 1 atm = 101.325 kPa; $P(CO_2)$ = CO_2 permeability; α = ideal CO_2/gas selectivity.
① Permeance measured in hollow-fiber membrane, GPU.

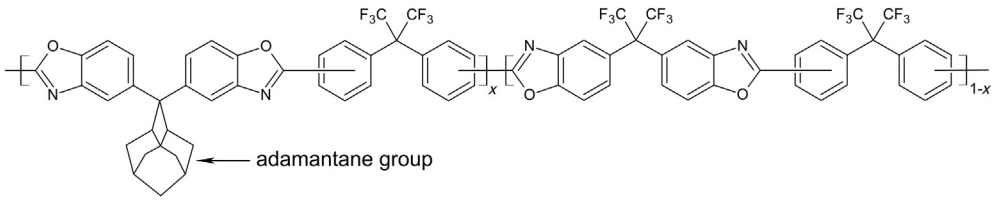

Fig. 9. Structure of 6FDA + bisAPAF with bulky ADHAB [93].

could not undergo the thermal rearrangement [100]. Different TR polymers can also be copolymerized as an attempt to combine the different transport features. Choi *et al.* synthesized a TR-PBO-*co*-PPL copolymer, which could be tuned to be highly CO_2 permeable by increasing the PBO content, or to be highly CO_2 selective *vs.* CH_4 by increasing the PPL content [101].

The cavity size and free volume of TR polymers can also be modified by grafting thermally labile moieties or introducing the spirobiindane center into the polymer backbones. Chung's group substituted the carboxylic acid group on the PI precursors with β-cyclodextrin (β-CD) or β-CD-ferrocene. The cyclodextrin was thermally labile and decomposed at 300–450 °C, which left micropores in the PI during the TR conversion [102,103]. This process is depicted in Fig. 10. Improved plasticization resistance and good mechanical strength were observed for this modified TR-α-PBO. Polymers with both TR and PIM segments were synthesized by Li *et al.* [104]. The main merit, however, was the improved mechanical properties compared to the pristine PIMs.

Due to the high temperature required by the TR conversion, the TR polymer membranes are typically synthesized by non-solvent induced phase inversion. Several asymmetric TR-β-PBO hollow-fiber membranes have been reported in the literature with a skin-layer thickness as thin as 200 nm [105,106]. A CO_2 permeance as high as 2500 GPU was reported with a CO_2/CH_4 selectivity of 22. Research efforts to reduce the thermal treatment temperature have also been reported. Guo *et al.* employed a 6FDA-2,2′-bis-[4-(3,4-dicarboxyphenoxy)phenyl]propane dianhydride precursor, which reduced the TR temperature by *ca.* 100 °C. A lower TR temperature improves the processability during the membrane formation [95]. Overall, as the glassy polymers with the highest chain rigidity, TR polymers are promising for high pressure, high temperature CO_2 separation applications. However, the high TR temperature and the associated membrane brittleness limit their scalability. Further research efforts on membrane formation are required for practical gas separations.

3.5. Iptycene-containing polymers

Two recently emerging building blocks for shape persisting macromolecular design are triptycene (Trip) and pentiptycene (Pent). These two molecules belong to the iptycene family, which is a class of three-dimensional molecules with arene units fused to the [2,2,2] bicyclooctatriene bridgehead system [107]. What makes iptycenes unique is that the clefts of the benzene "blades" form an internal free volume, which is comparable to the kinetic diameters of the light gases (Table 1). Due to its shape persisting nature, the internal free volume is not susceptible to collapse, thereby a less tendency for physical aging [108]. When incorporated into other polymer systems, the bulky iptycenes also disrupt the polymer chain packing and increase the overall free volume. A few iptycene-containing PEO and PIMs have been discussed in the previous sections [32,71]. In this section, polymers with iptycene units are reviewed in a more systematic manner. Table 6 summarizes the representative examples.

As suggested by Weidman *et al.*, these polymers can be grouped into three categories based on the backbone architecture: nonladder, semiladder and ladder polymers [117]. The iptycene-containing nonladder polymers are mainly polyimides with Trip or Pent built in the diamine and/or dianhydride monomers. One example is given by Cho *et al.*, where 6FDA was polymerized with 2,6-diaminotriptycene (DATRI) through a polycondensation reaction [109]. The fractional free volume increased to 0.226 from the 0.16–0.18 of 6FDA-based polyimides, and a CO_2 permeability of 189 Barrers with a CO_2/CH_4 selectivity of 30.5 was reported. Other iptycene-based diamines were also used, including DAT2 [88] and pentiptycene diamine (PPDA) [110]. The 6FDA can also be replaced with an iptycene-containing dihydride, *e.g.*, TPDAn, to synthesize polyimide fully based on the iptycene structures [111]. For this membrane, an interesting CO_2/CH_4 selectivity of 52 was reported. The highest CO_2/CH_4 selectivity, however, was registered by an iptycene-containing TR-PI, which demonstrated a selectivity as

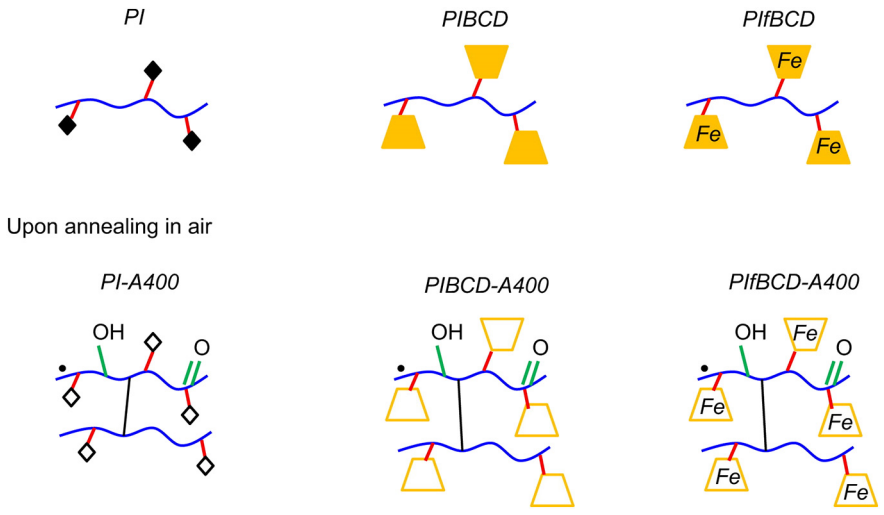

Fig. 10. Scheme of evolution of structural changes in the 6FDA polyimide containing carboxylic acid. (Adapted from Ref. [103] with permission from Elsevier.)

Table 6
Transport properties of selected iptycene-containing polymers

Strategy	Material	$p(CO_2)$/atm	T/°C	$P(CO_2)$/Barrer	α (CO_2/N_2)	α (CO_2/H_2)	α (CO_2/CH_4)
Nonladder	6FDA + DATRI [109]	1	35	189	23.3	0.73	30.5
	6FDA + DAT2 [88]	2	35	210	23.3	0.74	30
	6FDA + PPDA(CF_3) [110]	1	35	132	19	0.70	24
	TPDAn + 6FAP [111]	1	35	4.7	25	0	52
	TPHA-TC [112]	11	35	270	–	–	67
Semiladder	KAUST-PI-1 [113]	2	35	2389	22.3	0.60	22.8
	KAUST-PI-2 [113]	2	35	2071	21.1	0.87	20.5
	6FDA + PAF [114]	2	35	6.8	–	–	96
	TPDA + APAF [114]	2	35	46	–	–	53
	PBIBI + PPD [115]	1	25	137.2	27.8	–	36.2
Ladder	PIM-Trip-TB [116]	1	25	9709	15.4	1.2	10.7
	PIM-Btrip-TB [116]	1	25	13200	14.2	1.3	9.2

$p(CO_2)$ = CO_2 partial pressure, 1 atm = 101.325 kPa; $P(CO_2)$ = CO_2 permeability; α = ideal CO_2/gas selectivity.

high as 67 with a CO_2 permeability of 270 Barrers. Due to the relatively "soft" imide linkage, these nonladder polymers feature a better CO_2 selectivity than CO_2 permeability, although the permeability is at least one-order-of-magnitude higher than the traditional polyimides.

Most of the semiladder iptycene-contained polymers are synthesized by incorporating iptycene units into certain PIM-polyimide copolymers. The fused rings of PIM partially replace the single-bond connections in the polymer backbone, hence these polymers are termed as semiladder. A series of Trip-based PIM-polyimides were synthesized at KAUST, *e.g.*, KAUST-PI-1 and KAUST-PI-2, which showed high CO_2 permeabilities above 2000 Barrers with CO_2 *vs.* N_2 or CH_4 selectivities *ca.* 20. The polymer network can be further tightened up by the introduction of hydroxyl groups, which provides additional chain-to-chain interaction *via* hydrogen bonding. This modification method led to the synthesis of more selective PIM-polyimides, which showed a CO_2/CH_4 selectivity as high as 96 [114]. One semiladder polymer without the PIM structure was reported by Mao and Zhang, where the iptycene structure was built in the multi-amine monomer while the dianhydride monomer contained fused rings to stiffen the final polyimide backbone [115].

Lastly, ladder polymers were synthesized based on Tröger's base, a V-shape diamine described in Section 3.3 [116]. The introduction of iptycene structure increased the CO_2/CH_4 selectivity; the π–π interaction between the benzene rings on iptycene moderately reduced the free volume.

4. Facilitated Transport Membranes

In this section, the recent advances are discussed for polymers that are capable of selective CO_2 separation based on the facilitated transport mechanism. The most extensively studied amine carriers are discussed in Section 4.1. These amine-containing polymeric materials are further categorized based on whether amino groups are covalently bonded to the polymer backbone or freely dispersed in the polymer matrix. Other carriers, including various Brønsted bases, ionic liquids, and mimic enzymes, are discussed in Section 4.2.

4.1. Amine-containing membranes

Amines are the most exploited carriers for reactive CO_2 transport for three reasons. Firstly, with their importance in organic synthesis, amines encompass a rich structural variety [118]. The diverse synthesis routes provide certain easiness to impregnate amino groups into polymeric membranes. Secondly, the amine–CO_2 reactions are easily tunable to feature either fast reaction kinetics or high CO_2 loading capacity as briefed in Section 2.2. The balance of these two characteristics determines the overall facilitation effect. Lastly, the abundant experience in aqueous amine absorption for acid gas removal is transferable to the membrane synthesis. Polymeric facilitated transport membranes bear amines in two forms. The amino groups can be covalently bonded to the polymer backbone, which serve as the fixed-site carriers. The CO_2 molecules hop among neighboring amino groups, and the statistically more preferable hopping down the chemical potential gradient yields the facilitated CO_2 transport [24,25]. Alternatively, the amino groups can be incorporated in the polymer matrix *via* blending small molecule amines. These amines not only densify the amino group content in the membrane, but also can serve as mobile carriers for CO_2 transport, provided that the amine molecule size and the free volume of the polymer allow for certain carrier mobility. Table 7 categorizes the transport properties of selected amine-containing facilitated transport membranes based on the carrier types.

As for the fixed-site carriers, the transport properties of several polymers bearing amino groups have been studied, including polyvinylamine (PVAm) [119], poly(allylamine) (PAA) [24], poly(ethyleneimine) (PEI) [122], and chitosan [124], with a reducing density of primary amine groups. Limited by their low MW or high crystallinity, PAA, PEI, and chitosan are typically blended with other polymers. In this case, pristine or crosslinked poly(vinyl alcohol) (PVA) is the most common choice as the polymer matrix [24,122]. PVA not only enables the polymer mixture a suitable film forming ability. The hydrophilic nature of PVA also enhances the water retention ability, which eventually benefits the amine–CO_2 reaction [142,143]. Alternatively, PEO-based block copolymers have also been reported as a suitable polymer matrix. A blend of chitosan and Pebax® MH 1657 was reported by Liu *et al.*, which demonstrated a high CO_2 permeability of 2884 Barrers with a CO_2/CH_4 selectivity of 23.2 at 85 °C [124]. Unlike these polymers, PVAm has the highest amino group density. More importantly, the high MW PVAm can be easily synthesized *via* the polymerization of *N*-vinylformamide followed by an acid or base hydrolysis [144]. Consequently, PVAm is typically used alone as the polymer matrix. A CO_2 permeability of 103 Barrers as well as an unprecedented CO_2/CH_4 selectivity of 1143 was reported by Kim *et al.* [119].

These amine-containing polymers also provide a platform to carry out sophisticated amine chemistry. Zhao and Ho explored the steric hindrance effect in a solid state polymer system [24]. Bulky alkyl substitutes were incorporated on PAA *via* a series of S_N2 reactions. A membrane containing the moderately hindered poly-*N*-isopropylallylamine (PAA-C_3H_7) increased the CO_2 permeability to 297 Barrers from the 55 Barrers of the unmodified PAA membrane. A high CO_2/H_2 selectivity of 40 as well as a CO_2/N_2 selectivity of 341 was also achieved due to the enhanced CO_2 transport (Fig. 11). When the amine is sterically hindered, the carbamate ion formed by the nucleophile reaction with CO_2 is unstable due to the bulky alkyl group attached (Reaction (1) in Fig. 1). In this case, the carbamate ion can be easily hydrolyzed in the presence of water to form bicarbonate and regenerate a free amine (Reaction (2) in Fig. 1). Overall, 1 mol of CO_2 reacts with 1 mol of hindered amine; therefore, the CO_2 loading capacity is doubled compared to that of the unhindered amine. However, if the steric hindrance is too severe, the bulky alkyl group shields the nitrogen on the amino group from CO_2, thereby the reaction rate reduces. This tradeoff was

Table 7
Transport properties of selected amine-containing facilitated transport membranes

Strategy	Material	$p(CO_2)$/atm	T/°C	$P(CO_2)$/Barrer	α (CO_2/N_2)	α (CO_2/H_2)	α (CO_2/CH_4)
Fixed-site carrier	PVAm [119]	0.2	25	103	–	–	1143
	PVAm [120]	2	25	197	23.3	–	–
	PVA/PAA [24]	0.17	110	55	83	17	–
	PVA/PAA-C_3H_7 [24]	0.17	110	297	341	40	–
	PVA/PAA-C_4H_9 [24]	0.17	110	159	187	23	–
	PVA/PAA-$C(CH_3)_3$ [24]	0.17	110	119	179	34	–
	PVAm-CH_3 [121]	0.17	57	264	55	–	–
	PVAm-CH_3 [121]	0.04	102	6804	350	162	–
	PEI/PVA/PEG [122]	1	25	260	22	–	–
	PEI/PVA HF [123]	0.04	25	418	300	–	–
	Chitosan/Pebax® MH 1657 [124]	0.19	85	2884	65.3	–	23.2
	PVAm HF [125]	0.12	25	851①	500	–	–
	PVAm/PVA HF [126]	2	25	215①	–	–	45
	PVAm-PDA-PDMS [127]	0.3	25	1887①	83	–	–
	TMC + DNMDAm + DGBAmE [128]	0.2	30	1613①	138	–	–
	TMC + DAPP [129]	0.38	30	81①	–	7	23
	TMC + DNMDAm [130]	0.2	30	173①	70	–	37
Small molecule amine blending	SPBI-1/PAA/AIBA-K [131]	0.4	100	2539	–	65	–
	PAA/PVA/AIBA-K [132]	2.76	107	1296	–	87	–
	PVA/PAA-C_3H_7/AIBA-K [133]	0.17	110	6500	650	300	–
	PVA/Lupamin®/AIBA-K [134]	0.28	106	4100	–	245	–
	PVAm/EDA [135]	0.02	30	607①	106	–	–
	PVAm/MEA [136]	0.4	22	2661①	–	63	–
	PVAm/PZ [137]	0.02	22	6503①	277	–	–
	PVAm/K-Gly [138]	0.17	57	903①	173	–	–
	PVAm/Li-Gly [138]	0.17	57	1010①	202	–	–
	PVAm/PZ-Gly [138]	0.17	57	1100①	210	–	–
	PVAm/SDS/PZ-Gly [139]	0.17	57	1100①	140	–	–
Module	PVAm/PZ-Gly SW [140]	0.17	57	800①	200	–	–
	PVAm PF [141]	0.12	50	222①	300	–	–

$p(CO_2)$ = CO_2 partial pressure, 1 atm = 101.325 kPa; $P(CO_2)$ = CO_2 permeability; α = ideal CO_2/gas selectivity.
① Permeance measured in hollow-fiber or thin-film-composite membrane, GPU.

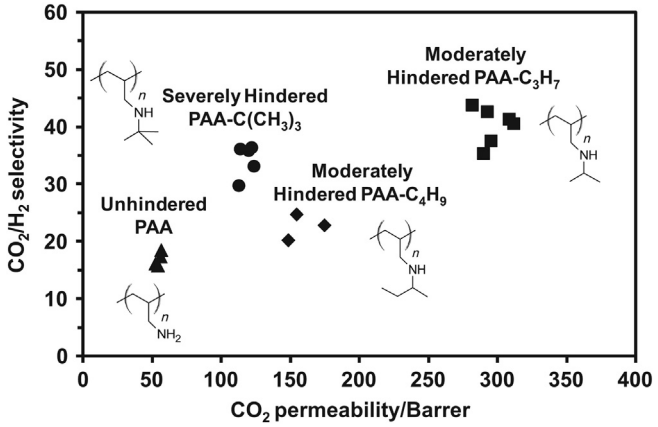

Fig. 11. CO_2/H_2 selectivity *versus* CO_2 permeability for membranes containing 70 wt% polyamines and 30 wt% crosslinked PVA at 110 °C and a feed pressure of 0.2 MPa. (Adapted from Ref. [24] with permission from Elsevier.)

also demonstrated by Zhao *et al.* for poly-*N*-tert-butylallylamine (PAA-C$(CH_3)_3$), which exhibited a reduced CO_2 permeability of 119 Barrers. A similar modification was conducted by Tong and Ho on PVAm, where poly(*N*-methyl-*N*-vinylamine) (PVAm-CH_3) showed a CO_2 permeability of 264 Barrers at 57 °C [121]. The permeation properties of this moderately hindered PVAm were affected by the temperature significantly. By increasing the temperature to 102 °C, the CO_2 permeability increased to 6804 Barrers with an impressive CO_2/H_2 selectivity of 162.

The abovementioned polymers also possess excellent processability. Membrane formation is much less challenging than most of the glassy polymers reviewed in Section 3. In most cases, water is a good solvent for the amine-containing polymers, and an ultrathin selective layer, *e.g.*, 100 nm, can be coated on proper substrate [127]. A thin selective layer can also be synthesized by a bottom-up approach. Wang's group has reported an interfacial polymerization method to prepare highly crosslinked amine-containing polymers by reacting multi-amines with trimesoyl chloride (TMC) [128–130]. A high CO_2 permeance of 1613 GPU with a CO_2/N_2 selectivity of 138 was registered [128].

Blending with small molecule amines is another facile approach to further enhance the facilitation effect of amine-containing membranes. Three categories of small molecule amines are widely adopted: amino alcohols [136], multi-amines [131], and amino acid salts [138]. Monoethanolamine (MEA) was incorporated in PVAm by Qiao *et al.* to achieve a CO_2 permeance of 2661 GPU with a CO_2/H_2 selectivity of 63. Another series of blended membranes were reported by Ho's group by adding the potassium salt of 2-aminoisobutyric acid (AIBA-K) in sulfonated polybenzimidazole (SPBI) [131], PAA-C_3H_7 [133], and PVAm [134], which demonstrated a CO_2/H_2 selectivity as high as 300 at 110 °C. These highly CO_2-selective membranes are interesting materials for H_2 purification. For CO_2/N_2 separation, piperazine (PZ) [137] and PZ-derivatives [139] have been proven as effective additives to PVAm membranes. The transport properties of these membranes largely depended on the detailed fabrication and testing conditions. However, a CO_2 permeance >1000 GPU and a CO_2/N_2 selectivity >140 were generally reported. This has attracted increasing attention of applying these membranes in post-combustion carbon capture.

For the superior processability and CO_2/N_2 selectivity, amine-containing membranes are among the few membrane materials that are in the stage of pilot-scale study for post-combustion carbon capture. The key concern for practical application, however, is the long-term stability in the presence of contaminants, especially SO_2. The more acidic SO_2 competes with CO_2 to react with amines, which might lead to membrane performance degradation. This issue has been intensively investigated. In general, a reduced CO_2 permeance was observed in the presence of ppm level SO_2 but not much for CO_2/N_2 selectivity; at moderate temperatures, *e.g.*, 57–67 °C, the separation performance was stable [145,146]. The PVAm-based membranes have been fabricated into spiral-wound (SW) and plate-and-frame (PF) membrane

modules for actual flue gas testing. Researchers at The Ohio State University (OSU) have tested their SW module at the National Carbon Capture Center (NCCC), Wilsonville, Alabama, U.S.A., with real flue gas, and a high CO_2 permeance of 800 GPU with a CO_2/N_2 selectivity of 200 has been reported [140]. The PF module developed by Hägg's group has been tested in the Nanoglowa EU project continuously for 6.5 months [141]. No performance degradation was observed under high level of SO_x and NO_x.

4.2. Other carriers for facilitated transport membranes

This section discusses the CO_2 carriers beyond amines. As listed in Table 8, these carriers are grouped into three categories: (1) base, (2) ionic liquid (IL) gel or poly(ionic liquid) (PIL), and (3) mimic enzyme.

Aside from amines, several other bases have been explored for their facilitation effect on CO_2 transport. These carriers either serve as a Brønsted base to react with CO_2, or catalyze the hydration reaction of CO_2 to form carbonate and bicarbonate. In terms of reaction kinetics, these basic carriers are incomparable to amines. However, they can be applied to several niche separation scenarios where the harsh conditions exclude the use of amines. The hydroxide OH^- group has been reported as an efficient CO_2 carrier at high temperature by Vakharia *et al.* [147]. Different forms of quaternary ammonium ion were chosen as the counterion due to their relatively good thermal and oxidative stabilities, which were introduced in the membrane by poly(diallyldimethylammonium hydroxide) (PDADMQ-OH) and tetramethylammonium hydroxide (TMAOH). The PDADMQ-OH was also replaced with poly(diallyldimethylammonium fluoride) (PDADMQ-F) in the same study, where the fluoride ion catalyzed the CO_2 hydration reaction. Overall, a CO_2 permeance of >50 GPU and a high CO_2/H_2 selectivity of >100 were reported at 120 °C in the presence of CO and O_2. A similar quaternary ammonium-based polyelectrolyte was used by Li *et al.* to copolymerize with PVAm [151]. However, CO_3^{2-} was chosen as the anion to react with CO_2 as well as to reduce the copolymer crystallinity. Facilitation effect on CO_2 was also reported for carboxylate ion [152,153]. These much weaker Brønsted bases were investigated mainly for their oxidative stability in the presence of O_2. Lastly, organic super bases, *e.g.*, amidine [149] and guanidine [150], have also been employed as CO_2 carriers. A facile method to graft guanidine to polyaniline (PANI) membrane was demonstrated by Blinova and Svec [150]. Provided sufficient hydration, the guanidine-modified PANI showed a high CO_2 permeability of 2460 Barrers with a CO_2/CH_4 selectivity of 540, which is interesting for natural gas sweetening.

Room temperature ILs bearing CO_2-reactive functional groups are another class of emerging materials for CO_2 separation. A combination of the high CO_2 solubility and the facilitated transport effect provides ILs not only high CO_2 selectivity, but also high CO_2 permeability in the membrane form [163]. The various IL-based supported liquid membranes are out of the scope of this review. Here, only free-standing IL membranes are discussed. Two methods have been developed to anchor ILs in a free-standing membrane: (1) polymerize IL-containing monomers to form PIL and (2) embed IL into a compatible polymer matrix to form IL gel. Noble's group has used several bis(epoxide)-functionalized IL monomers to crosslink with tris(2-aminoethyl) amine (TAEA) [154,155,164]. The tertiary amine linkages formed by the crosslinking facilitates the CO_2 transport, yielding a CO_2 permeability as high as 900 Barrers with a CO_2/N_2 selectivity of 138 at room temperature. The carrier site can also be incorporated into the IL units, *e.g.*, tetrabutylphosphonium glycine ($[P_{4444}][Gly]$), serine ($[P_{4444}][SER]$), lysine ($[P_{4444}][Lys]$), and proline ($[P_{4444}][Pro]$) [157]. In this case, the IL carriers are typically embedded in a gel network to form an "elastomer-like" film at room temperature. One example is given by Moghadam *et al.*, where $[P_{222(101)}][Inda]$ was synthesized by neutralizing a phosphonium hydroxide by indazole [159]. This IL was embedded in a polymer network formed by poly(methacryloylamino propyl trimethylammonium chloride) and poly(dimethylacrylamide) (PMAPTAC/PDMAAm). In the final ion-gel membrane, $[P_{222(101)}][Inda]$ served as the carrier, and a CO_2 permeability of 7569 Barrers was reported at 100 °C.

As mentioned earlier, the fluoride ion is capable of catalyzing the hydration of CO_2. A similar functionality is achieved by carbonic anhydrase (CA), a metalloenzyme in biological processes. The activity of CA derives from a Zn^{2+} coordinate to three histidine groups, known as α-CA, or to two cysteine groups and a histidine group, known as β-CA [165]. These active sites have been artificially constructed by complexing Zn^{2+} with imidazole groups in poly(*N*-vinyl imidazole) (Fig. 12 (a)) or impregnate a Zn atom into cyclen (Fig. 12 (b)) [160–162]. Depending on the hosting polymer, these mimic enzymes facilitated the CO_2 transport, and a high CO_2/N_2 selectivity above 80 was reported. It is worth noting that the activities of the mimic enzymes are about an order of magnitude lower than those of the native enzymes. Further studies are needed in this area, *e.g.*, changing Zn^{2+} to Cd^{2+} to mimic γ-CA, an enzyme with an even lower activation energy for the CO_2 hydration reaction [166].

5. Conclusions and Outlook

The recent advances in polymeric membranes for CO_2 capture are reviewed in terms of the material design and membrane formation.

Table 8
Transport properties of selected facilitated transport membranes

Strategy	Material	$p(CO_2)$/atm	T/°C	$P(CO_2)$/Barrer	α (CO_2/N_2)	α (CO_2/H_2)	α (CO_2/CH_4)
Base	PVA/PDADMQ-OH/TMAOH [147]	0.12	120	93①	–	58	–
	PVA/PDADMQ-F/TMAOH [147]	0.12	120	140①	–	108	–
	TPQPOH [148]	1	25	1090	275		
	PS-*b*-PEO/amidine [149]	1	20	216①	2	–	–
	PANI/guanidine [150]	0.12	NA	3460	–	–	540
	Poly(DADMACA-*co*-VAm) [151]	0.15	25	1870①	160	29	84
	Poly(AAS-*co*-AAm) [152]	0.15	25	95①	63	–	–
	TMC + DAmBS + DGBAmE [153]	0.15	25	5831①	86	–	–
IL gel/PIL	[EMIM][DCA] + TAEA [154]	0.5	25	900	138	–	–
	[EMIM][Tf_2N] + TAEA [155]	0.4	25	525	–	–	18
	[TETA][Tfa] + PEG [156]	0.2	25	117	131.1	–	70.3
	$[P_{4444}][Gly]$/PVP [157]	0.025	100	10205	230	–	–
	$[P_{4444}][Pro]$/PAMPS/PDMAAm [158]	0.001	30	52000	8100	–	–
	$[P_{222(101)}][Inda]$/PMAPTAC/PDMAAm [159]	0.1	100	7569	210	–	–
Mimic enzyme	Zn-cyclen/PVA [160]	0.12	25	255.5①	107	–	–
	Zn-cyclen/PVA [161]	0.12	25	362.9①	120	–	–
	PVI-Zn^{2+} [162]	0.17	25	1122①	83	–	–

$p(CO_2)$ = CO_2 partial pressure, 1 atm = 101.325 kPa; $P(CO_2)$ = CO_2 permeability; α = ideal CO_2/gas selectivity.
① Permeance measured in thin-film-composite membrane, GPU.

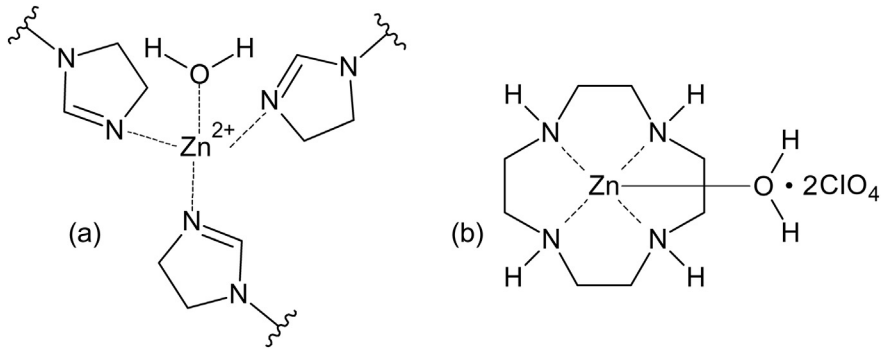

Fig. 12. Two types of mimic enzymes: (a) Zn^{2+}–imidazole complex for α-CA; (b) Zn-cyclen for β -CA.

Opportunities and challenges in practical applications are also discussed, including post-combustion carbon capture (CO_2/N_2), hydrogen purification (CO_2/H_2), and natural gas sweetening (CO_2/CH_4). To compare the various polymeric membrane materials, selected data from Tables 2–8 are plotted in Fig. 13, along with the 2008 Robeson upper bound. A Robeson upper bound does not exist when plotting CO_2/H_2 selectivity against CO_2 permeability. Inverting the H_2/CO_2 Robeson upper bound gives the CO_2/H_2 lower bound. Therefore, the theoretical upper bound for rubbery polymers predicted by Freeman is used [11,167]. The final remarks and outlook are summarized below for these three gas pairs.

(1) The shape persisting glassy polymers define the highly permeable end of the CO_2/N_2 upper bound. However, the low CO_2 partial pressure in the coal-derived flue gases requires a significant CO_2/N_2 selectivity to achieve >95% CO_2 purity at 90% CO_2 capture. The abundant techno-economic analyses generally agree that a minimal selectivity of 50 is needed for membrane to compete with aqueous amine absorption [50,168,169]. In this case, the PEO-based membranes and amine-based facilitated transport membranes provide sufficient permselectivity to allow for practical membrane process design. Another advantage of these two classes of polymers is their processability. A thin selective layer *ca.* 100 nm has been demonstrated in flat-sheet and hollow-fiber composite membranes, and suitable membrane modules in commercial configurations have also been fabricated. Their technical potential is also reflected in the pilot-scale field tests conducted in the U.S. and Europe. An on-going research focus is to further boost the CO_2 permeance exceeding 3000 GPU. The reproducible and cost-effective fabrication of ultrathin selective layer is crucial. In addition, an ultrathin and ultra-permeable selective layer calls for innovations in substrate synthesis [170].

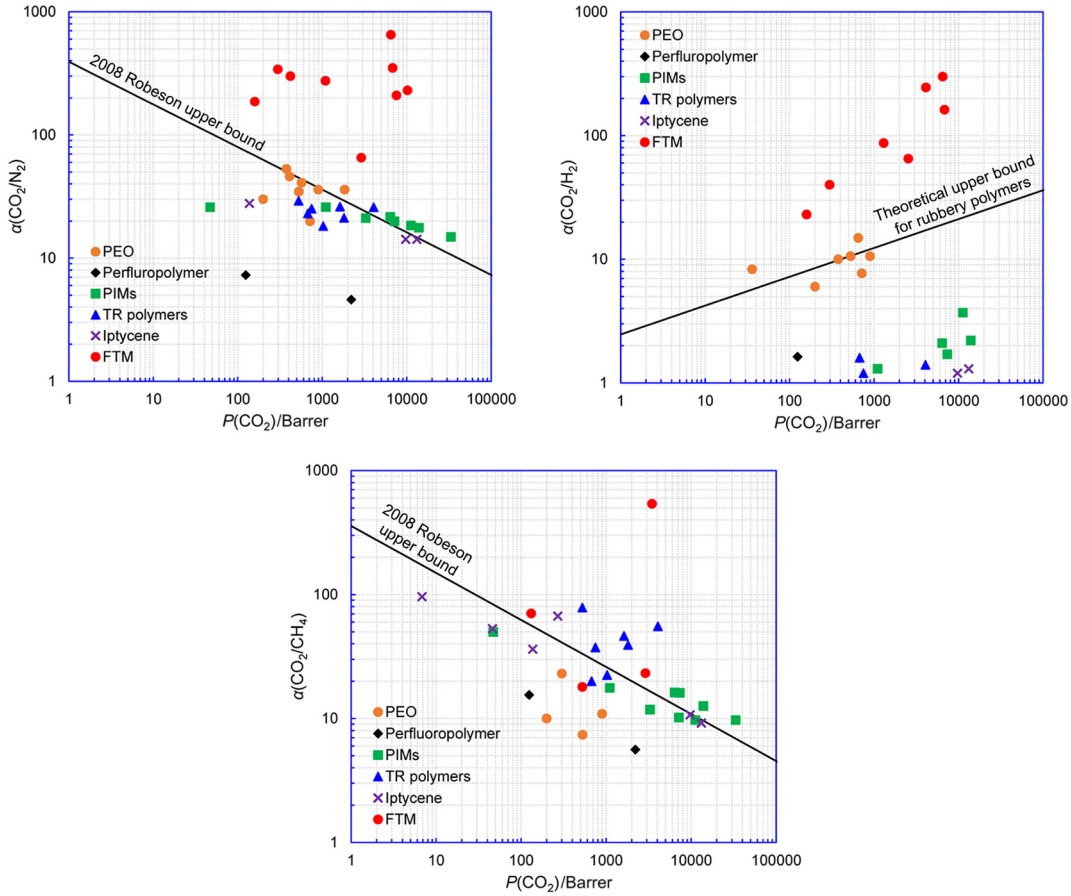

Fig. 13. Transport properties of selected polymeric materials *vs.* 2008 Robeson upper bound [13] or the theoretical upper bound for rubbery polymers in CO_2/H_2 separation [167].

The nanoscale pore structure of the substrate affects the composite membrane separation performance. The Knudsen diffusion in the substrate and the pore restriction at the selective layer-substrate interface can account for a significant portion of the transport resistance [171,172]. Novel isoporous substrate self-assembled by block copolymers might lead the research efforts in membrane formation. The application of facilitated transport membranes is not limited to decarbonizing the coal-derived flue gases. Their unprecedented CO_2/N_2 selectivity is a necessity for carbon capture from gas sources with even lower CO_2 concentration, *e.g.*, natural gas-derived flue gas, coal mine gas, and residual flue gas after the primary carbon capture.

(2) Once again, PEO-based membranes and facilitated transport membranes are the only feasible materials for selective CO_2 removal from hydrogen. The reviewed polymers with rigid chains are more suitable for H_2-selective membrane synthesis, although they face the competition against several other glassy polymers featuring high H_2/CO_2 selectivity, *e.g.*, polybenzimidazole and crosslinked polyimide [173]. The required CO_2/H_2 selectivity for pre-combustion carbon capture is not well-defined. However, the high CO_2/H_2 selectivity demonstrated by the amine-containing facilitated transport membranes is expected to be beneficial for enhancing the H_2 recovery upon a high degree of CO_2 removal, thus an overall higher energy efficiency. More importantly, these facilitated transport membranes have been reported to be stable at elevated temperatures >100 °C in the presence of H_2S [133]. These characteristics eliminate the intensive cooling and pre-treatment in pre-combustion carbon capture, which are usually required for solution-diffusion membranes. One disadvantage of facilitated transport membrane is the deteriorated CO_2 permeability and CO_2/H_2 selectivity at high CO_2 partial pressure due to the carrier saturation phenomenon [136]. For a given CO_2 partial pressure, the carrier saturation can be mitigated by increasing the carrier content. However, the hosting polymer should be able to form a mechanically robust yet highly permeable network to accommodate the carrier molecules. The design principle of polymer network for IL-gel membranes might shed light on polymer synthesis to host other type of CO_2-carriers. In addition, other CO_2-philic moieties can be blended with the CO_2-carriers to enhance the CO_2 solubility at high CO_2 partial pressure. For facilitated transport membranes, the membrane stability at high temperature and pressure needs to be demonstrated. Opportunities in several niche applications are also available, *e.g.*, H_2 purification and recycling from fuel cell discharge gas [174]. Novel membrane design, however, is needed to accommodate for the different operating conditions and contaminants.

(3) TR polymers, perfluoropolymers, PIMs, and facilitated transport membranes cover a wide feasible range for CO_2/CH_4 separation. TR polymers and perfluoropolymers are of special interest since their transport properties are well above the 2008 Robeson upper bound. The chemical resistance of perfluoropolymers is well suited for natural gas sweetening. One concern, however, is the membrane plasticization in the presence of water, which affects both TR polymers and perfluoropolymers. Further studies in polymer properties and innovative engineering are needed to realize the separation performances in practical applications. In addition, several modified polyimides have been reported recently with notable tolerance to CO_2 and H_2O plasticization, where the polymer chain mobility was restricted by introducing bulky Trip linkages in the polymer backbone [109] or grafting bulky —CF_3 as pendent groups [175]. Amine- and guanidine-containing facilitated transport membranes can take advantage of the high water content in some crude natural gases. The likely high H_2O permeance of these membranes can also dehydrate the natural gas upon CO_2 removal. Carrier saturation at high feed pressure is the main challenge for facilitated transport membranes in CO_2/CH_4 separation.

Nomenclature

D_i	diffusion coefficient of gas component CO_2
D_j	diffusion coefficient of another gas component (N_2, H_2 or CH_4)
i	gas component CO_2
j	another gas component (N_2, H_2 or CH_4)
P_i	permeability of species i
S_i	solubility coefficient of gas component CO_2
S_j	solubility coefficient of another gas component (N_2, H_2 or CH_4)
α_{ij}	ideal selectivity of species i over species j

Acknowledgments

We would like to thank José D. Figueroa of National Energy Technology Laboratory for providing helpful discussion and input. We would like to gratefully acknowledge the U.S. Department of Energy/National Energy Technology Laboratory (DE-FE0026919) and the Ohio Development Services Agency (OOE-CDO-D-13-05 and OER-CDO-D-15-09) for their financial support of this work. This work was partly supported by the U.S. Department of Energy under Award Number DE-FE0026919 with substantial involvement of the National Energy Technology Laboratory, Pittsburgh, PA, USA.

References

[1] B. Metz, O. Davidson, H. De Coninck, M. Loos, L. Meyer, IPCC special report on carbon dioxide capture and storage, Prepared by Working Group III of the Intergovernmental Panel on Climate Change, IPCC, Cambridge University Press, Cambridge, United Kingdom and New York, USA, 2005.
[2] K. Ramasubramanian, Y. Zhao, W.S.W. Ho, CO_2 capture and H_2 purification: Prospects for CO_2-selective membrane processes, *AICHE J.* 59 (4) (2013) 1033–1045.
[3] W.S.W. Ho, K.K. Sirkar, Membrane Handbook, Chapman & Hall, New York, 1992, Kluwer Academic Publishers, Boston, reprint edition, 2001.
[4] J. Black, Cost and Performance Baseline for Fossil Energy Plants Volume 1: Bituminous Coal and Natural Gas to Electricity Final Report, 2nd ed. National Energy Technology Laboratory, November, 2010.
[5] L. Zhao, E. Riensche, L. Blum, D. Stolten, How gas separation membrane competes with chemical absorption in postcombustion capture, *Energy Procedia* 4 (2011) 629–636.
[6] L. Zhao, E. Riensche, L. Blum, D. Stolten, Multi-stage gas separation membrane processes used in post-combustion capture: Energetic and economic analyses, *J. Membr. Sci.* 359 (1) (2010) 160–172.
[7] T. Fout, A. Zoelle, D. Keairns, M. Turner, M. Woods, N. Kuehn, V. Shah, V. Chou, L. Pinkerton, J. Black, Cost and Performance Baseline for Fossil Energy Plants Volume 1b: Bituminous Coal (IGCC) to Electricity Revision 2b—Year Dollar Update, United States Departmeant of Energy, Washington, DC, USA, 2015.
[8] J.D. Wind, D.R. Paul, W.J. Koros, Natural gas permeation in polyimide membranes, *J. Membr. Sci.* 228 (2) (2004) 227–236.
[9] S. Harms, K. Rätzke, F. Faupel, N. Chaukura, P. Budd, W. Egger, L. Ravelli, Aging and free volume in a polymer of intrinsic microporosity (PIM-1), *J. Adhes.* 88 (7) (2012) 608–619.
[10] L. Robeson, B. Freeman, D. Paul, B. Rowe, An empirical correlation of gas permeability and permselectivity in polymers and its theoretical basis, *J. Membr. Sci.* 341 (1–2) (2009) 178–185.
[11] B.D. Freeman, Basis of permeability/selectivity tradeoff relations in polymeric gas separation membranes, *Macromolecules* 32 (2) (1999) 375–380.
[12] L.M. Robeson, Correlation of separation factor versus permeability for polymeric membranes, *J. Membr. Sci.* 62 (2) (1991) 165–185.
[13] L.M. Robeson, The upper bound revisited, *J. Membr. Sci.* 320 (1) (2008) 390–400.
[14] S. Janakiram, M. Ahmadi, Z. Dai, L. Ansaloni, L. Deng, Performance of nanocomposite membranes containing 0D to 2D nanofillers for CO_2 separation: A review, *Membranes* 8 (2) (2018) 24.
[15] M. Wang, Z. Wang, S. Zhao, J. Wang, S. Wang, Recent advances on mixed matrix membranes for CO_2 separation, *Chin. J. Chem. Eng.* 25 (2017) 1581–1597.
[16] J. Wijmans, R. Baker, The solution–diffusion model: A review, *J. Membr. Sci.* 107 (1) (1995) 1–21.
[17] V.T. Stannett, Simple gases, in: J. Crank, G.S. Park (Eds.), Diffusion in Polymers, Academic Press, New York, New York 1968, pp. 41–73.
[18] G. Dong, H. Li, V. Chen, Challenges and opportunities for mixed-matrix membranes for gas separation, *J. Mater. Chem. A* 1 (15) (2013) 4610–4630.
[19] V. Bondar, B. Freeman, I. Pinnau, Gas transport properties of poly (ether-*b*-amide) segmented block copolymers, *J. Polym. Sci. B Polym. Phys.* 38 (15) (2000) 2051–2062.

[20] J.D. Goddard, J.S. Schultz, S.R. Suchdeo, Facilitated transport via carrier-mediated diffusion in membranes: Part II. Mathematical aspects and analyses, *AIChE J.* 20 (4) (1974) 625–645.

[21] J.H. Meldon, P. Stroeve, C.E. Gregoire, Facilitated transport of carbon dioxide: A review, *Chem. Eng. Commun.* 16 (1–6) (1982) 263–300.

[22] P. Danckwerts, The reaction of CO_2 with ethanolamines, *Chem. Eng. Sci.* 34 (4) (1979) 443–446.

[23] P.V. Kortunov, M. Siskin, L.S. Baugh, D.C. Calabro, In situ nuclear magnetic resonance mechanistic studies of carbon dioxide reactions with liquid amines in aqueous systems: New insights on carbon capture reaction pathways, *Energy Fuel* 29 (9) (2015) 5919–5939.

[24] Y. Zhao, W.S.W. Ho, Steric hindrance effect on amine demonstrated in solid polymer membranes for CO_2 transport, *J. Membr. Sci.* 415 (2012) 132–138.

[25] E. Cussler, R. Aris, A. Bhown, On the limits of facilitated diffusion, *J. Membr. Sci.* 43 (2) (1989) 149–164.

[26] F. Rindfleisch, T.P. DiNoia, M.A. McHugh, Solubility of polymers and copolymers in supercritical CO_2, *J. Phys. Chem.* 100 (38) (1996) 15581–15587.

[27] H. Lin, B.D. Freeman, Materials selection guidelines for membranes that remove CO_2 from gas mixtures, *J. Mol. Struct.* 739 (1–3) (2005) 57–74.

[28] L. Zhu, B.R. Mimnaugh, Q. Ge, R.P. Quirk, S.Z. Cheng, E.L. Thomas, B. Lotz, B.S. Hsiao, F. Yeh, L. Liu, Hard and soft confinement effects on polymer crystallization in microphase separated cylinder-forming PEO-*b*-PS/PS blends, *Polymer* 42 (21) (2001) 9121–9131.

[29] W. Yave, A. Car, S.S. Funari, S.P. Nunes, K.-V. Peinemann, CO_2-philic polymer membrane with extremely high separation performance, *Macromolecules* 43 (1) (2009) 326–333.

[30] S.H. Ahn, S.J. Kim, D.K. Roh, H.-K. Lee, B. Jung, J.H. Kim, Controlling gas permeability of a graft copolymer membrane using solvent vapor treatment, *Macromol. Res.* 22 (2) (2014) 160–164.

[31] S.R. Reijerkerk, A.C. IJzer, K. Nijmeijer, A. Arun, R.J. Gaymans, M. Wessling, Subambient temperature CO_2 and light gas permeation through segmented block copolymers with tailored soft phase, *ACS Appl. Mater. Interfaces* 2 (2) (2010) 551–560.

[32] S. Luo, K.A. Stevens, J.S. Park, J.D. Moon, Q. Liu, B.D. Freeman, R. Guo, Highly CO_2-selective gas separation membranes based on segmented copolymers of poly(ethylene oxide) reinforced with pentiptycene-containing polyimide hard segments, *ACS Appl. Mater. Interfaces* 8 (3) (2016) 2306–2317.

[33] J. Xia, S. Liu, T.-S. Chung, Effect of end groups and grafting on the CO_2 separation performance of poly(ethylene glycol) based membranes, *Macromolecules* 44 (19) (2011) 7727–7736.

[34] W. Yave, H. Huth, A. Car, C. Schick, Peculiarity of a CO_2-philic block copolymer confined in thin films with constrained thickness: "A super membrane for CO_2-capture", *Energy Environ. Sci.* 4 (11) (2011) 4656–4661.

[35] B. Xue, X. Li, L. Gao, M. Gao, Y. Wang, L. Jiang, CO_2-selective free-standing membrane by self-assembly of a UV-crosslinkable diblock copolymer, *J. Mater. Chem.* 22 (21) (2012) 10918–10923.

[36] S. Feng, J. Ren, K. Hua, H. Li, X. Ren, M. Deng, Poly(amide-12-*b*-ethylene oxide)/polyethylene glycol blend membranes for carbon dioxide separation, *Sep. Purif. Technol.* 116 (2013) 25–34.

[37] W. Yave, A. Car, K.-V. Peinemann, Nanostructured membrane material designed for carbon dioxide separation, *J. Membr. Sci.* 350 (1–2) (2010) 124–129.

[38] S.R. Reijerkerk, M. Wessling, K. Nijmeijer, Pushing the limits of block copolymer membranes for CO_2 separation, *J. Membr. Sci.* 378 (1–2) (2011) 479–484.

[39] Y. Chen, B. Wang, L. Zhao, P. Dutta, W.S.W. Ho, New Pebax®/zeolite Y composite membranes for CO_2 capture from flue gas, *J. Membr. Sci.* 495 (2015) 415–423.

[40] J.M. Scofield, P.A. Gurr, J. Kim, Q. Fu, S.E. Kentish, G.G. Qiao, Development of novel fluorinated additives for high performance CO_2 separation thin-film composite membranes, *J. Membr. Sci.* 499 (2016) 191–200.

[41] H. Lin, E. Van Wagner, J.S. Swinnea, B.D. Freeman, S.J. Pas, A.J. Hill, S. Kalakkunnath, D.S. Kalika, Transport and structural characteristics of crosslinked poly(ethylene oxide) rubbers, *J. Membr. Sci.* 276 (1–2) (2006) 145–161.

[42] H. Lin, E. Van Wagner, R. Raharjo, B.D. Freeman, I. Roman, High-performance polymer membranes for natural-gas sweetening, *Adv. Mater.* 18 (1) (2006) 39–44.

[43] V.A. Kusuma, B.D. Freeman, S.L. Smith, A.L. Heilman, D.S. Kalika, Influence of TRIS-based co-monomer on structure and gas transport properties of cross-linked poly (ethylene oxide), *J. Membr. Sci.* 359 (1–2) (2010) 25–36.

[44] I. Taniguchi, T. Kai, S. Duan, S. Kazama, H. Jinnai, A compatible crosslinker for enhancement of CO_2 capture of poly(amidoamine) dendrimer-containing polymeric membranes, *J. Membr. Sci.* 475 (2015) 175–183.

[45] T. Sakaguchi, F. Katsura, A. Iwase, T. Hashimoto, CO_2-permselective membranes of crosslinked poly(vinyl ether)s bearing oxyethylene chains, *Polymer* 55 (6) (2014) 1459–1466.

[46] S. Quan, S. Li, Z. Wang, X. Yan, Z. Guo, L. Shao, A bio-inspired CO_2-philic network membrane for enhanced sustainable gas separation, *J. Mater. Chem. A* 3 (26) (2015) 13758–13766.

[47] G.K. Kline, J.R. Weidman, Q. Zhang, R. Guo, Studies of the synergistic effects of crosslink density and crosslink inhomogeneity on crosslinked PEO membranes for CO_2-selective separations, *J. Membr. Sci.* 544 (2017) 25–34.

[48] A.A. Salih, C. Yi, H. Peng, B. Yang, L. Yin, W. Wang, Interfacially polymerized polyetheramine thin film composite membranes with PDMS inter-layer for CO_2 separation, *J. Membr. Sci.* 472 (2014) 110–118.

[49] S. Li, Z. Wang, C. Zhang, M. Wang, F. Yuan, J. Wang, S. Wang, Interfacially polymerized thin film composite membranes containing ethylene oxide groups for CO_2 separation, *J. Membr. Sci.* 436 (2013) 121–131.

[50] T.C. Merkel, H. Lin, X. Wei, R. Baker, Power plant post-combustion carbon dioxide capture: An opportunity for membranes, *J. Membr. Sci.* 359 (1) (2010) 126–139.

[51] H. Lin, S.M. Thompson, A. Serbanescu-Martin, J.G. Wijmans, K.D. Amo, K.A. Lokhandwala, T.C. Merkel, Dehydration of natural gas using membranes. Part I: Composite membranes, *J. Membr. Sci.* 413 (2012) 70–81.

[52] T.C. Merkel, I. Pinnau, R. Prabhakar, B.D. Freeman, Gas and vapor transport properties of perfluoropolymers, in: B.D. Freeman, Y. Yampolskii, I. Pinnau (Eds.), Material Science of Membranes for Gas and Vapor Separation, John Wiley & Sons, 2006.

[53] I. Pinnau, L.G. Toy, Gas and vapor transport properties of amorphous perfluorinated copolymer membranes based on 2,2-bistrifluoromethyl-4,5-difluoro-1,3-dioxole/tetrafluoroethylene, *J. Membr. Sci.* 109 (1) (1996) 125–133.

[54] Y. Okamoto, H. Zhang, F. Mikes, Y. Koike, Z. He, T.C. Merkel, New perfluorodioxolane-based membranes for gas separations, *J. Membr. Sci.* 471 (2014) 412–419.

[55] M. Fang, Y. Okamoto, Y. Koike, Z. He, T.C. Merkel, Gas separation membranes prepared with copolymers of perfluoro(2-methylene-4,5-dimethyl-1,3-dioxlane) and chlorotrifluoroethylene, *J. Fluor. Chem.* 188 (2016) 18–22.

[56] T. Merkel, V. Bondar, K. Nagai, B. Freeman, Y.P. Yampolskii, Gas sorption, diffusion, and permeation in poly(2,2-bis(trifluoromethyl)-4,5-difluoro-1,3-dioxole-*co*-tetrafluoroethylene), *Macromolecules* 32 (25) (1999) 8427–8440.

[57] A.Y. Alentiev, V. Shantarovich, T. Merkel, V. Bondar, B. Freeman, Y.P. Yampolskii, Gas and vapor sorption, permeation, and diffusion in glassy amorphous Teflon AF1600, *Macromolecules* 35 (25) (2002) 9513–9522.

[58] V. Arcella, A. Ghielmi, G. Tommasi, High performance perfluoropolymer films and membranes, *Ann. N. Y. Acad. Sci.* 984 (1) (2003) 226–244.

[59] M. Yavari, M. Fang, H. Nguyen, T.C. Merkel, H. Lin, Y. Okamoto, Dioxolane-based perfluoropolymers with superior membrane gas separation properties, *Macromolecules* 51 (7) (2018) 2489–2497.

[60] M. Fang, Z. He, T.C. Merkel, Y. Okamoto, High-performance perfluorodioxolane copolymer membranes for gas separation with tailored selectivity enhancement, *J. Mater. Chem. A* 6 (2018) 652–658.

[61] R.R. Tiwari, Z.P. Smith, H. Lin, B. Freeman, D. Paul, Gas permeation in thin films of "high free-volume" glassy perfluoropolymers: Part I. Physical aging, *Polymer* 55 (22) (2014) 5788–5800.

[62] R.R. Tiwari, Z.P. Smith, H. Lin, B. Freeman, D. Paul, Gas permeation in thin films of "high free-volume" glassy perfluoropolymers: Part II. CO_2 plasticization and sorption, *Polymer* 61 (2015) 1–14.

[63] M. Yavari, T. Le, H. Lin, Physical aging of glassy perfluoropolymers in thin film composite membranes. Part I. Gas transport properties, *J. Membr. Sci.* 525 (2017) 387–398.

[64] M. Yavari, S. Maruf, Y. Ding, H. Lin, Physical aging of glassy perfluoropolymers in thin film composite membranes. Part II. Glass transition temperature and the free volume model, *J. Membr. Sci.* 525 (2017) 399–408.

[65] P.M. Budd, B.S. Ghanem, S. Makhseed, N.B. McKeown, K.J. Msayib, C.E. Tattershall, Polymers of intrinsic microporosity (PIMs): Robust, solution-processable, organic nanoporous materials, *Chem. Commun.* 0 (2) (2004) 230–231.

[66] P.M. Budd, N.B. McKeown, D. Fritsch, Free volume and intrinsic microporosity in polymers, *J. Mater. Chem.* 15 (20) (2005) 1977–1986.

[67] N.B. McKeown, P.M. Budd, Polymers of intrinsic microporosity (PIMs): Organic materials for membrane separations, heterogeneous catalysis and hydrogen storage, *Chem. Soc. Rev.* 35 (8) (2006) 675–683.

[68] P.M. Budd, N.B. McKeown, B.S. Ghanem, K.J. Msayib, D. Fritsch, L. Starannikova, N. Belov, O. Sanfirova, Y. Yampolskii, V. Shantarovich, Gas permeation parameters and other physicochemical properties of a polymer of intrinsic microporosity: Polybenzodioxane PIM-1, *J. Membr. Sci.* 325 (2) (2008) 851–860.

[69] P.M. Budd, K.J. Msayib, C.E. Tattershall, B.S. Ghanem, K.J. Reynolds, N.B. McKeown, D. Fritsch, Gas separation membranes from polymers of intrinsic microporosity, *J. Membr. Sci.* 251 (1–2) (2005) 263–269.

[70] C.G. Bezzu, M. Carta, A. Tonkins, J.C. Jansen, P. Bernardo, F. Bazzarelli, N.B. McKeown, A spirobifluorene-based polymer of intrinsic microporosity with improved performance for gas separation, *Adv. Mater.* 24 (44) (2012) 5930–5933.

[71] I. Rose, C.G. Bezzu, M. Carta, B. Comesaña-Gándara, E. Lasseuguette, M.C. Ferrari, P. Bernardo, G. Clarizia, A. Fuoco, J.C. Jansen, Polymer ultrapermeability from the inefficient packing of 2D chains, *Nat. Mater.* 16 (9) (2017) 932.

[72] M. Carta, R. Malpass-Evans, M. Croad, Y. Rogan, J.C. Jansen, P. Bernardo, F. Bazzarelli, N.B. McKeown, An efficient polymer molecular sieve for membrane gas separations, *Science* 339 (6117) (2013) 303–307.

[73] M. Carta, M. Croad, R. Malpass-Evans, J.C. Jansen, P. Bernardo, G. Clarizia, K. Friess, M. Lanč, N.B. McKeown, Triptycene induced enhancement of membrane gas selectivity for microporous Tröger's base polymers, *Adv. Mater.* 26 (21) (2014) 3526–3531.

[74] Y. Rogan, L. Starannikova, V. Ryzhikh, Y. Yampolskii, P. Bernardo, F. Bazzarelli, J.C. Jansen, N.B. McKeown, Synthesis and gas permeation properties of novel spirobisindane-based polyimides of intrinsic microporosity, *Polym. Chem.* 4 (13) (2013) 3813–3820.

[75] Y. Rogan, R. Malpass-Evans, M. Carta, M. Lee, J.C. Jansen, P. Bernardo, G. Clarizia, E. Tocci, K. Friess, M. Lanč, A highly permeable polyimide with enhanced selectivity for membrane gas separations, *J. Mater. Chem. A* 2 (14) (2014) 4874–4877.

[76] N. Alaslai, X. Ma, B. Ghanem, Y. Wang, F. Alghunaimi, I. Pinnau, Synthesis and characterization of a novel microporous dihydroxyl-functionalized triptycene-diamine-based polyimide for natural gas membrane separation, *Macromol. Rapid Commun.* 38 (18) (2017).

[77] M. Carta, P. Bernardo, G. Clarizia, J.C. Jansen, N.B. McKeown, Gas permeability of hexaphenylbenzene based polymers of intrinsic microporosity, *Macromolecules* 47 (23) (2014) 8320–8327.

[78] Q. Song, S. Cao, R.H. Pritchard, B. Ghalei, S.A. Al-Muhtaseb, E.M. Terentjev, A.K. Cheetham, E. Sivaniah, Controlled thermal oxidative crosslinking of polymers of intrinsic microporosity towards tunable molecular sieve membranes, *Nat. Commun.* 5 (2014) 4813.

[79] Q. Song, S. Cao, P. Zavala-Rivera, L.P. Lu, W. Li, Y. Ji, S.A. Al-Muhtaseb, A.K. Cheetham, E. Sivaniah, Photo-oxidative enhancement of polymeric molecular sieve membranes, *Nat. Commun.* 4 (2013) 1918.

[80] T.O. McDonald, R. Akhtar, C.H. Lau, T. Ratvijitvech, G. Cheng, R. Clowes, D.J. Adams, T. Hasell, A.I. Cooper, Using intermolecular interactions to crosslink PIM-1 and modify its gas sorption properties, *J. Mater. Chem. A* 3 (9) (2015) 4855–4864.

[81] W.F. Yong, T.-S. Chung, Miscible blends of carboxylated polymers of intrinsic microporosity (cPIM-1) and Matrimid, *Polymer* 59 (2015) 290–297.

[82] L. Hao, P. Li, T.-S. Chung, PIM-1 as an organic filler to enhance the gas separation performance of Ultem polyetherimide, *J. Membr. Sci.* 453 (2014) 614–623.

[83] L. Yang, Z. Tian, X. Zhang, X. Wu, Y. Wu, Y. Wang, D. Peng, S. Wang, H. Wu, Z. Jiang, Enhanced CO_2 selectivities by incorporating CO_2-philic PEG–POSS into polymers of intrinsic microporosity membrane, *J. Membr. Sci.* 543 (2017) 69–78.

[84] T. Mitra, R.S. Bhavsar, D.J. Adams, P.M. Budd, A.I. Cooper, PIM-1 mixed matrix membranes for gas separations using cost-effective hypercrosslinked nanoparticle fillers, *Chem. Commun.* 52 (32) (2016) 5581–5584.

[85] M.L. Jue, V. Breedveld, R.P. Lively, Defect-free PIM-1 hollow fiber membranes, *J. Membr. Sci.* 530 (2017) 33–41.

[86] Z.G. Wang, X. Liu, D. Wang, J. Jin, Tröger's base-based copolymers with intrinsic microporosity for CO_2 separation and effect of Tröger's base on separation performance, *Polym. Chem.* 5 (8) (2014) 2793–2800.

[87] N.B. McKeown, Polymers of intrinsic microporosity, *ISRN Mater. Sci.* 2012 (2012).

[88] F. Alghunaimi, B. Ghanem, N. Alaslai, R. Swaidan, E. Litwiller, I. Pinnau, Gas permeation and physical aging properties of iptycene diamine-based microporous polyimides, *J. Membr. Sci.* 490 (2015) 321–327.

[89] M.M. Khan, G. Bengtson, S. Shishatskiy, B.N. Gacal, M.M. Rahman, S. Neumann, V. Filiz, V. Abetz, Cross-linking of polymer of intrinsic microporosity (PIM-1) via nitrene reaction and its effect on gas transport property, *Eur. Polym. J.* 49 (12) (2013) 4157–4166.

[90] H.B. Park, C.H. Jung, Y.M. Lee, A.J. Hill, S.J. Pas, S.T. Mudie, E. Van Wagner, B.D. Freeman, D.J. Cookson, Polymers with cavities tuned for fast selective transport of small molecules and ions, *Science* 318 (5848) (2007) 254–258.

[91] S. Kim, Y.M. Lee, Rigid and microporous polymers for gas separation membranes, *Prog. Polym. Sci.* 43 (2015) 1–32.

[92] H. Wang, T.-S. Chung, The evolution of physicochemical and gas transport properties of thermally rearranged polyhydroxyamide (PHA), *J. Membr. Sci.* 385 (2011) 86–95.

[93] C. Aguilar-Lugo, C. Álvarez, Y.M. Lee, J.G. de la Campa, A.n.E. Lozano, Thermally rearranged polybenzoxazoles containing bulky adamantyl groups from *ortho*-substituted precursor copolyimides, *Macromolecules* 51 (5) (2018) 1605–1619.

[94] S.H. Han, N. Misdan, S. Kim, C.M. Doherty, A.J. Hill, Y.M. Lee, Thermally rearranged (TR) polybenzoxazole: Effects of diverse imidization routes on physical properties and gas transport behaviors, *Macromolecules* 43 (18) (2010) 7657–7667.

[95] R. Guo, D.F. Sanders, Z.P. Smith, B.D. Freeman, D.R. Paul, J.E. McGrath, Synthesis and characterization of thermally rearranged (TR) polymers: Effect of glass transition temperature of aromatic poly (hydroxyimide) precursors on TR process and gas permeation properties, *J. Mater. Chem. A* 1 (19) (2013) 6063–6072.

[96] S.H. Han, J.E. Lee, K.-J. Lee, H.B. Park, Y.M. Lee, Highly gas permeable and microporous polybenzimidazole membrane by thermal rearrangement, *J. Membr. Sci.* 357 (1–2) (2010) 143–151.

[97] M. Calle, C.M. Doherty, A.J. Hill, Y.M. Lee, Cross-linked thermally rearranged poly (benzoxazole-*co*-imide) membranes for gas separation, *Macromolecules* 46 (20) (2013) 8179–8189.

[98] M. Calle, H.J. Jo, C.M. Doherty, A.J. Hill, Y.M. Lee, Cross-linked thermally rearranged poly (benzoxazole-*co*-imide) membranes prepared from *ortho*-hydroxycopolyimides containing pendant carboxyl groups and gas separation properties, *Macromolecules* 48 (8) (2015) 2603–2613.

[99] H.J. Jo, C.Y. Soo, G. Dong, Y.S. Do, H.H. Wang, M.J. Lee, J.R. Quay, M.K. Murphy, Y.M. Lee, Thermally rearranged poly (benzoxazole-*co*-imide) membranes with superior mechanical strength for gas separation obtained by tuning chain rigidity, *Macromolecules* 48 (7) (2015) 2194–2202.

[100] C.A. Scholes, C.P. Ribeiro, S.E. Kentish, B.D. Freeman, Thermal rearranged poly (benzoxazole-*co*-imide) membranes for CO_2 separation, *J. Membr. Sci.* 450 (2014) 72–80.

[101] J.I. Choi, C.H. Jung, S.H. Han, H.B. Park, Y.M. Lee, Thermally rearranged (TR) poly (benzoxazole-*co*-pyrrolone) membranes tuned for high gas permeability and selectivity, *J. Membr. Sci.* 349 (1–2) (2010) 358–368.

[102] Y. Xiao, T.-S. Chung, Grafting thermally labile molecules on cross-linkable polyimide to design membrane materials for natural gas purification and CO_2 capture, *Energy Environ. Sci.* 4 (1) (2011) 201–208.

[103] M.L. Chua, Y.C. Xiao, T.-S. Chung, Modifying the molecular structure and gas separation performance of thermally labile polyimide-based membranes for enhanced natural gas purification, *Chem. Eng. Sci.* 104 (2013) 1056–1064.

[104] S. Li, H.J. Jo, S.H. Han, C.H. Park, S. Kim, P.M. Budd, Y.M. Lee, Mechanically robust thermally rearranged (TR) polymer membranes with spirobisindane for gas separation, *J. Membr. Sci.* 434 (2013) 137–147.

[105] S. Kim, S.H. Han, Y.M. Lee, Thermally rearranged (TR) polybenzoxazole hollow fiber membranes for CO_2 capture, *J. Membr. Sci.* 403 (2012) 169–178.

[106] K.T. Woo, J. Lee, G. Dong, J.S. Kim, Y.S. Do, W.-S. Hung, K.-R. Lee, G. Barbieri, E. Drioli, Y.M. Lee, Fabrication of thermally rearranged (TR) polybenzoxazole hollow fiber membranes with superior CO_2/N_2 separation performance, *J. Membr. Sci.* 490 (2015) 129–138.

[107] Y. Jiang, C.F. Chen, Recent developments in synthesis and applications of triptycene and pentiptycene derivatives, *Eur. J. Org. Chem.* 2011 (32) (2011) 6377–6403.

[108] T.M. Long, T.M. Swager, Using "internal free volume" to increase chromophore alignment, *J. Am. Chem. Soc.* 124 (15) (2002) 3826–3827.

[109] Y.J. Cho, H.B. Park, High performance polyimide with high internal free volume elements, *Macromol. Rapid Commun.* 32 (7) (2011) 579–586.

[110] S. Luo, Q. Liu, B. Zhang, J.R. Wiegand, B.D. Freeman, R. Guo, Pentiptycene-based polyimides with hierarchically controlled molecular cavity architecture for efficient membrane gas separation, *J. Membr. Sci.* 480 (2015) 20–30.

[111] S. Luo, J.R. Wiegand, P. Gao, C.M. Doherty, A.J. Hill, R. Guo, Molecular origins of fast and selective gas transport in pentiptycene-containing polyimide membranes and their physical aging behavior, *J. Membr. Sci.* 518 (2016) 100–109.

[112] S. Luo, J.R. Wiegand, B. Kazanowska, C.M. Doherty, K. Konstas, A.J. Hill, R. Guo, Finely tuning the free volume architecture in iptycene-containing polyimides for highly selective and fast hydrogen transport, *Macromolecules* 49 (9) (2016) 3395–3405.

[113] B.S. Ghanem, R. Swaidan, E. Litwiller, I. Pinnau, Ultra-microporous triptycene-based polyimide membranes for high-performance gas separation, *Adv. Mater.* 26 (22) (2014) 3688–3692.

[114] R. Swaidan, B. Ghanem, E. Litwiller, I. Pinnau, Effects of hydroxyl-functionalization and sub-T_g thermal annealing on high pressure pure- and mixed-gas CO_2/CH_4 separation by polyimide membranes based on 6FDA and triptycene-containing dianhydrides, *J. Membr. Sci.* 475 (2015) 571–581.

[115] H. Mao, S. Zhang, Synthesis, characterization, and gas transport properties of novel iptycene-based poly[bis(benzimidazobenzisoquinolinones)], *Polymer* 55 (1) (2014) 102–109.

[116] I. Rose, M. Carta, R. Malpass-Evans, M.-C. Ferrari, P. Bernardo, G. Clarizia, J.C. Jansen, N.B. McKeown, Highly permeable benzotriptycene-based polymer of intrinsic microporosity, *ACS Macro Lett.* 4 (9) (2015) 912–915.

[117] J.R. Weidman, R. Guo, The use of iptycenes in rational macromolecular design for gas separation membrane applications, *Ind. Eng. Chem. Res.* 56 (15) (2017) 4220–4236.

[118] S.A. Lawrence, Amines: Synthesis, Properties and Applications, Cambridge University Press, 2004.

[119] T.J. Kim, B. Li, M.B. Hägg, Novel fixed-site-carrier polyvinylamine membrane for carbon dioxide capture, *J. Polym. Sci. B Polym. Phys.* 42 (23) (2004) 4326–4336.

[120] M. Sandru, T.-J. Kim, M.-B. Hägg, High molecular fixed-site-carrier PVAm membrane for CO_2 capture, *Desalination* 240 (1–3) (2009) 298–300.

[121] Z. Tong, W.S.W. Ho, New sterically hindered polyvinylamine membranes for CO_2 separation and capture, *J. Membr. Sci.* 543 (2017) 202–211.

[122] S.B. Hamouda, Q.T. Nguyen, D. Langevin, S. Roudesli, Poly(vinylalcohol)/poly (ethyleneglycol)/poly(ethyleneimine) blend membranes — Structure and CO_2 facilitated transport, *C. R. Chim.* 13 (3) (2010) 372–379.

[123] M.S.A. Rahaman, L. Zhang, L.-H. Cheng, X.-H. Xu, H.-L. Chen, Capturing carbon dioxide from air using a fixed carrier facilitated transport membrane, *RSC Adv.* 2 (24) (2012) 9165–9172.

[124] Y. Liu, S. Yu, H. Wu, Y. Li, S. Wang, Z. Tian, Z. Jiang, High permeability hydrogel membranes of chitosan/polyether-block-amide blends for CO_2 separation, *J. Membr. Sci.* 469 (2014) 198–208.

[125] M. Sandru, S.H. Haukebø, M.-B. Hägg, Composite hollow fiber membranes for CO_2 capture, *J. Membr. Sci.* 346 (1) (2010) 172–186.

[126] L. Deng, M.-B. Hägg, Fabrication and evaluation of a blend facilitated transport membrane for CO_2/CH_4 separation, *Ind. Eng. Chem. Res.* 54 (44) (2015) 11139–11150.

[127] P. Li, Z. Wang, W. Li, Y. Liu, J. Wang, S. Wang, High-performance multilayer composite membranes with mussel-inspired polydopamine as a versatile molecular bridge for CO_2 separation, *ACS Appl. Mater. Interfaces* 7 (28) (2015) 15481–15493.

[128] S. Li, Z. Wang, X. Yu, J. Wang, S. Wang, High-performance membranes with multi-permselectivity for CO_2 separation, *Adv. Mater.* 24 (24) (2012) 3196–3200.

[129] W. He, Z. Wang, W. Li, S. Li, Z. Bai, J. Wang, S. Wang, Cyclic tertiary amino group containing fixed carrier membranes for CO_2 separation, *J. Membr. Sci.* 476 (2015) 171–181.

[130] X. Yu, Z. Wang, Z. Wei, S. Yuan, J. Zhao, J. Wang, S. Wang, Novel tertiary amino containing thin film composite membranes prepared by interfacial polymerization for CO_2 capture, *J. Membr. Sci.* 362 (1–2) (2010) 265–278.

[131] H. Bai, W.S.W. Ho, New carbon dioxide-selective membranes based on sulfonated polybenzimidazole (SPBI) copolymer matrix for fuel cell applications, *Ind. Eng. Chem. Res.* 48 (5) (2008) 2344–2354.

[132] R. Xing, W.S.W. Ho, Crosslinked polyvinylalcohol–polysiloxane/fumed silica mixed matrix membranes containing amines for CO_2/H_2 separation, *J. Membr. Sci.* 367 (1–2) (2011) 91–102.

[133] Y. Zhao, W.S.W. Ho, CO_2-selective membranes containing sterically hindered amines for CO_2/H_2 separation, *Ind. Eng. Chem. Res.* 52 (26) (2012) 8774–8782.

[134] V. Vakharia, K. Ramasubramanian, W.S.W. Ho, An experimental and modeling study of CO_2-selective membranes for IGCC syngas purification, *J. Membr. Sci.* 488 (2015) 56–66.

[135] S. Yuan, Z. Wang, Z. Qiao, M. Wang, J. Wang, S. Wang, Improvement of CO_2/N_2 separation characteristics of polyvinylamine by modifying with ethylenediamine, *J. Membr. Sci.* 378 (1–2) (2011) 425–437.

[136] Z. Qiao, Z. Wang, S. Yuan, J. Wang, S. Wang, Preparation and characterization of small molecular amine modified PVAm membranes for CO_2/H_2 separation, *J. Membr. Sci.* 475 (2015) 290–302.

[137] Z. Qiao, Z. Wang, C. Zhang, S. Yuan, Y. Zhu, J. Wang, S. Wang, PVAm–PIP/PS composite membrane with high performance for CO_2/N_2 separation, *AIChE J.* 59 (1) (2013) 215–228.

[138] Y. Chen, L. Zhao, B. Wang, P. Dutta, W.S.W. Ho, Amine-containing polymer/zeolite Y composite membranes for CO_2/N_2 separation, *J. Membr. Sci.* 497 (2016) 21–28.

[139] Y. Chen, W.S.W. Ho, High-molecular-weight polyvinylamine/piperazine glycinate membranes for CO_2 capture from flue gas, *J. Membr. Sci.* 514 (2016) 376–384.

[140] W. Salim, V. Vakharia, Y. Chen, D. Wu, Y. Han, W.S.W. Ho, Fabrication and field testing of spiral-wound membrane modules for CO_2 capture from flue gas, *J. Membr. Sci.* 556 (2018) 126–137.

[141] M. Sandru, T.-J. Kim, W. Capala, M. Huijbers, M.-B. Hägg, Pilot scale testing of polymeric membranes for CO_2 capture from coal fired power plants, *Energy Procedia* 37 (2013) 6473–6480.
[142] J. Huang, J. Zou, W.S.W. Ho, Carbon dioxide capture using a CO_2-selective facilitated transport membrane, *Ind. Eng. Chem. Res.* 47 (4) (2008) 1261–1267.
[143] J. Zou, W.S.W. Ho, CO_2-selective polymeric membranes containing amines in crosslinked poly(vinyl alcohol), *J. Membr. Sci.* 286 (1) (2006) 310–321.
[144] R. Pelton, Polyvinylamine: A tool for engineering interfaces, *Langmuir* 30 (51) (2014) 15373–15382.
[145] D. Wu, C. Sun, P.K. Dutta, W.W. Ho, SO_2 interference on separation performance of amine-containing facilitated transport membranes for CO_2 capture from flue gas, *J. Membr. Sci.* 534 (2017) 33–45.
[146] S. Li, Z. Wang, W. He, C. Zhang, H. Wu, J. Wang, S. Wang, Effects of minor SO_2 on the transport properties of fixed carrier membranes for CO_2 capture, *Ind. Eng. Chem. Res.* 53 (18) (2014) 7758–7767.
[147] V. Vakharia, W. Salim, M. Gasda, W.S.W. Ho, Oxidatively stable membranes for CO_2 separation and H_2 purification, *J. Membr. Sci.* 533 (2017) 220–228.
[148] L. Xiong, S. Gu, K.O. Jensen, Y.S. Yan, Facilitated transport in hydroxide-exchange membranes for post-combustion CO_2 separation, *ChemSusChem* 7 (1) (2014) 114–116.
[149] Y. Wang, Y. Shang, X. Li, T. Tian, L. Gao, L. Jiang, Fabrication of CO_2 facilitated transport channels in block copolymer through supramolecular assembly, *Polymers* 6 (5) (2014) 1403–1413.
[150] N.V. Blinova, F. Svec, Functionalized polyaniline-based composite membranes with vastly improved performance for separation of carbon dioxide from methane, *J. Membr. Sci.* 423 (2012) 514–521.
[151] P. Li, Z. Wang, Y. Liu, S. Zhao, J. Wang, S. Wang, A synergistic strategy via the combination of multiple functional groups into membranes towards superior CO_2 separation performances, *J. Membr. Sci.* 476 (2015) 243–255.
[152] M. Wang, Z. Wang, J. Wang, Y. Zhu, S. Wang, An antioxidative composite membrane with the carboxylate group as a fixed carrier for CO_2 separation from flue gas, *Energy Environ. Sci.* 4 (10) (2011) 3955–3959.
[153] M. Wang, Z. Wang, S. Li, C. Zhang, J. Wang, S. Wang, A high performance antioxidative and acid resistant membrane prepared by interfacial polymerization for CO_2 separation from flue gas, *Energy Environ. Sci.* 6 (2) (2013) 539–551.
[154] W.M. McDanel, M.G. Cowan, N.O. Chisholm, D.L. Gin, R.D. Noble, Fixed-site-carrier facilitated transport of carbon dioxide through ionic-liquid-based epoxy-amine ion gel membranes, *J. Membr. Sci.* 492 (2015) 303–311.
[155] K. Friess, M. Lanč, K. Pilnáček, V. Fíla, O. Vopička, Z. Sedláková, M.G. Cowan, W.M. McDanel, R.D. Noble, D.L. Gin, CO_2/CH_4 separation performance of ionic-liquid-based epoxy-amine ion gel membranes under mixed feed conditions relevant to biogas processing, *J. Membr. Sci.* 528 (2017) 64–71.
[156] Z. Dai, L. Ansaloni, D.L. Gin, R.D. Noble, L. Deng, Facile fabrication of CO_2 separation membranes by cross-linking of poly (ethylene glycol) diglycidyl ether with a diamine and a polyamine-based ionic liquid, *J. Membr. Sci.* 523 (2017) 551–560.
[157] S. Kasahara, E. Kamio, A. Yoshizumi, H. Matsuyama, Polymeric ion-gels containing an amino acid ionic liquid for facilitated CO_2 transport media, *Chem. Commun.* 50 (23) (2014) 2996–2999.
[158] F. Moghadam, E. Kamio, H. Matsuyama, High CO_2 separation performance of amino acid ionic liquid-based double network ion gel membranes in low CO_2 concentration gas mixtures under humid conditions, *J. Membr. Sci.* 525 (2017) 290–297.
[159] F. Moghadam, E. Kamio, T. Yoshioka, H. Matsuyama, New approach for the fabrication of double-network ion-gel membranes with high CO_2/N_2 separation performance based on facilitated transport, *J. Membr. Sci.* 530 (2017) 166–175.
[160] M. Saeed, L. Deng, CO_2 facilitated transport membrane promoted by mimic enzyme, *J. Membr. Sci.* 494 (2015) 196–204.
[161] M. Saeed, L. Deng, Carbon nanotube enhanced PVA-mimic enzyme membrane for post-combustion CO_2 capture, *Int. J. Greenhouse Gas Control* 53 (2016) 254–262.
[162] K. Yao, Z. Wang, J. Wang, S. Wang, Biomimetic material — poly(*N*-vinylimidazole)–zinc complex for CO_2 separation, *Chem. Commun.* 48 (12) (2012) 1766–1768.
[163] M.G. Cowan, D.L. Gin, R.D. Noble, Poly (ionic liquid)/ionic liquid ion-gels with high "free" ionic liquid content: Platform membrane materials for CO_2/light gas separations, *Acc. Chem. Res.* 49 (4) (2016) 724–732.
[164] W.M. McDanel, M.G. Cowan, T.K. Carlisle, A.K. Swanson, R.D. Noble, D.L. Gin, Cross-linked ionic resins and gels from epoxide-functionalized imidazolium ionic liquid monomers, *Polymer* 55 (16) (2014) 3305–3313.
[165] J.K. Yong, G.W. Stevens, F. Caruso, S.E. Kentish, The use of carbonic anhydrase to accelerate carbon dioxide capture processes, *J. Chem. Technol. Biotechnol.* 90 (1) (2015) 3–10.
[166] Y. Xu, L. Feng, P.D. Jeffrey, Y. Shi, F.M. Morel, Structure and metal exchange in the cadmium carbonic anhydrase of marine diatoms, *Nature* 452 (7183) (2008) 56.
[167] H. Lin, E. Van Wagner, B.D. Freeman, L.G. Toy, R.P. Gupta, Plasticization-enhanced hydrogen purification using polymeric membranes, *Science* 311 (5761) (2006) 639–642.
[168] D. Bocciardo, M.-C. Ferrari, S. Brandani, Modelling and multi-stage design of membrane processes applied to carbon capture in coal-fired power plants, *Energy Procedia* 37 (2013) 932–940.
[169] K. Ramasubramanian, H. Verweij, W.S.W. Ho, Membrane processes for carbon capture from coal-fired power plant flue gas: A modeling and cost study, *J. Membr. Sci.* 421 (2012) 299–310.
[170] D. Wu, L. Zhao, V.K. Vakharia, W. Salim, W.S.W. Ho, Synthesis and characterization of nanoporous polyethersulfone membrane as support for composite membrane in CO_2 separation: From lab to pilot scale, *J. Membr. Sci.* 510 (2016) 58–71.
[171] G.Z. Ramon, M.C. Wong, E.M. Hoek, Transport through composite membrane, part 1: Is there an optimal support membrane? *J. Membr. Sci.* 415 (2012) 298–305.
[172] M. Kattula, K. Ponnuru, L. Zhu, W. Jia, H. Lin, E.P. Furlani, Designing ultrathin film composite membranes: The impact of a gutter layer, *Sci. Rep.* 5 (2015).
[173] R.P. Singh, K.A. Berchtold, H_2 selective membranes for precombustion carbon capture, Novel Materials for Carbon Dioxide Mitigation Technology, Elsevier 2015, pp. 177–206.
[174] W. Salim, V. Vakharia, K.K. Chen, M. Gasda, W.S.W. Ho, Oxidatively stable borate-containing membranes for H_2 purification for fuel cells, *J. Membr. Sci.* 562 (2018) 9–17.
[175] G. Liu, N. Li, S.J. Miller, D. Kim, S. Yi, Y. Labreche, W.J. Koros, Molecularly designed stabilized asymmetric hollow fiber membranes for aggressive natural gas separation, *Angew. Chem.* 128 (44) (2016) 13958–13962.